Technical Report

TR-01-35

U and Pb isotope analysis of uraninite and galena by ion microprobe

Lena Z Evins, Torbjörn Sunde, Hans Schöberg
Laboratory for Isotope Geology, Swedish Museum of Natural History

Mostafa Fayek
University of Tennessee, Department of Geological Sciences

October 2001

Svensk Kärnbränslehantering AB
Swedish Nuclear Fuel
and Waste Management Co
Box 5864
SE-102 40 Stockholm Sweden
Tel 08-459 84 00
+46 8 459 84 00
Fax 08-661 57 19
+46 8 661 57 19

U and Pb isotope analysis of uraninite and galena by ion microprobe

Lena Z Evins, Torbjörn Sunde, Hans Schöberg
Laboratory for Isotope Geology, Swedish Museum of Natural History

Mostafa Fayek
University of Tennessee, Department of Geological Sciences

October 2001

Abstract

Accurate isotopic analysis of minerals by ion microprobe, or SIMS (Secondary Ion Mass Spectrometry) usually requires a standard to correct for instrumental mass bias effects that occur during analysis. We have calibrated two uraninite crystals and one galena crystal to be used as ion probe standards. As part of this study we describe the analytical procedures and problems encountered while trying to establish fractionation factors for U and Pb isotopes measured in galena and uraninite. Only the intra-element isotopic mass fractionation is considered and not the inter-element fractionation.

Galena and uraninite were analysed with TIMS (Thermal Ionisation Mass Spectrometry) prior to SIMS. One uraninite crystal (P88) comes from Sweden and is ca 900 Ma old, the other from Maine, USA (LAMNH-30222) and is ca 350 Ma old. The galena sample comes from the Paleoproterozoic ore district Bergslagen in Sweden. SIMS analyses were performed at two different laboratories: the NORDSIM facility in Stockholm, which has a high resolution Cameca IMS 1270 ion microprobe, and the Oak Ridge National Laboratory (ORNL) in Tennessee, which has a Cameca IMS 4f ion microprobe.

The results show that during the analysis of galena, Pb isotopes fractionate in favour of the lighter isotope by as much as 0.5%/amu. A Pb isotope fractionation factor for uraninite was more difficult to calculate, probably due to the formation of hydride interferences encountered during analysis with the Cameca IMS 1270 ion microprobe. However, drying the sample in vacuum prior to analysis, and using high-energy filtering and a cold trap during analysis can minimise these hydride interferences. A large fractionation of U isotopes of ca 1.4%/amu in favour of the lighter isotope was calculated for uraninite.

Sammanfattning

Med jonmikrosond, eller SIMS (Secondary Ion Mass Spectrometry), kan man utföra noggranna analyser av olika minerals isotopiska sammansättning. Ofta förekommer dock instrumentell massfraktionering under analysen, för vilken man måste korrigera mätresultaten. Detta kräver vanligtvis en standard av samma mineral som man ska analysera. Vi har utvärderat och kalibrerat två uraninitkristaller och en blyglanskristall för detta ändamål. Vi beskriver också de analytiska procedurer och problem som förekom under försöken att etablera fraktioneringsfaktorer för uran-och blyisotoper uppmätta i uraninit och blyglans. I denna studie diskuterar vi enbart massfraktionering mellan isotoper av samma element, och inte den fraktionering som förekommer mellan olika element.

Blyglans och uraninit analyserades med TIMS (Thermal Ionisation Mass Spectrometry) före SIMS. En uraninitkristall (P88) kommer från Sverige och är ca. 900 Ma gammal, den andra kommer från Maine, USA, och är ca 350 Ma gammal. Blyglanskristallen kommer från det paleoproterozoiska malmdistriktet Bergslagen i Sverige. Jonmikro-sondanalyser utfördes vid två olika laboratorier: NORDSIM i Stockholm, som har en högupplösande Cameca IMS 1270, och Oak Ridge National Laboratory (ORNL) i Tennessee, som har en Cameca IMS 4f.

Resultaten visar att under blyglansanalyser fraktionerar blyisotoper till fördel för den lättare isotopen så mycket som 0,5 %/amu. En fraktioneringsfaktor för Pb i uraninit var svårare att bestämma, troligen beroende på interferenser med blyhydrider. Svårigheter med hydrider påträffades under analys med jonmikrosonden Cameca IMS 1270. Mängden hydridinterferenser kan minskas genom att torka ut provet i vakuum före analys, använda en köldfälla i provkammaren, samt att utnyttja en metod kallad högenergi-filtrering under analysens gång. Uranisotoper visade sig fraktionera kraftigt, ca 1,4 %/amu till fördel för den lättare isotopen, vid analys av uraninit.

Table of contents

1 Introduction

Secondary Ion Mass Spectrometry (SIMS) is an important tool for the geochronologist. The method allows *in situ* isotopic analysis on individual mineral grains, eliminating the need for dissolution and chemical processing which is fundamental for the conventional TIMS (Thermal Ionisation Mass Spectrometry) method. SIMS analysis involves bombardment of the solid sample by a primary ion beam, which sputters material from the sample. The sputtered material forms a plasma just above the sample surface, and secondary ions from this plasma are accelerated into the mass spectrometer.

The intrinsic mass dependent bias introduced during measurement of isotope ratios is referred to as instrumental mass fractionation (IMF). This effect is common to all forms of isotopic analysis and can limit measurement accuracy if appropriate corrections are not implemented. In ion microprobe analysis, IMF is corrected for by comparing measurements of a chemically and isotopically homogenous mineral standard that is compositionally similar to the unknown. The similarity between the standard and the unknown is critical because of the existences of compositionally dependent fractionations that are commonly referred to as matrix effects /e.g., Valley et al., 1998/. Ion microprobe results from the standard are compared to its accepted isotopic composition in order to compute a correction factor that is applied to the unknowns measured during the same analysis session.

A variety of processes combine to produce the observed IMF during SIMS analysis. These include sputtering and ionisation /Shroeer et al., 1973; Sigmund, 1969; Williams, 1979; Yu and Lang, 1986/, secondary ion transmission /Shimizu and Hart, 1982/ and detection /Lyon et al., 1994; Valley and Graham, 1991/. The contributors to the IMF that depend most strongly upon sample characteristics (i.e., sputtering and ionisation) are the source of the matrix effects. While isotopic fractionation in single-element samples /Shimizu and Hart, 1982; Slodzian et al., 1980; Weathers et al., 1993/ are well-documented and qualitatively explicable by secondary ion production theory, the physics of matrix effects is relatively unknown and must be calibrated empirically.

During zircon U-Pb analyses by SIMS, the fractionation between Pb isotopes is considered negligible, and the main use of a zircon U-Pb standard is to determine the correct inter-elemental (U/Pb) isotopic ratios. A study of Pb isotope fractionation in standard glasses during ion probe analysis did not reveal any resolvable mass discrimination of Pb isotopes /Belshaw et al., 1994/. However, this does not have to be true for galena and uraninite, due to matrix effects as well as the higher precision arising from the high concentration of Pb in the sample. In fact, fractionation of Pb isotopes during galena analysis by ion microprobe was shown to be almost 0.5%/amu /Meddaugh et al., 1982/. Uraninite analyses have shown a fractionation of Pb isotopes of ca 0.35%/amu /Holliger, 1988/, and a very large fractionation of ca 2%/amu of the U isotopes /Holliger, 1992/. Thus, it is important to establish the intra-elemental fractionation on standards in order to measure accurate isotopic ratios of the mineral in question.

The purpose of this report is to describe the analytical procedures for accurate ion microprobe analyses of U and Pb isotopes from galena and uraninite. We have obtained two chemically homogenous uraninite crystals and one galena crystal. The U and Pb isotopic composition of these potential standards was verified by TIMS. This report will

not discuss the inter-elemental fractionation, caused by difference in ion yield for different elements in the same matrix, but rather focus on the fractionation between isotopes of Pb and U. It should be noted that in the following text, the word fractionation will be used in a wide sense, meaning simply the deviation of the SIMS measured values from the “true” values, measured by TIMS.

2 Analytical techniques

2.1 Sample selection and preparation

The samples listed in Table 2-1 were selected for initial examination for homogeneity and alteration.

Table 2-1. Table of the samples investigated in association with uraninite and galena analyses on the ion microprobe.

Mineral	Sample number	Locality	Country	Host rock
Uraninite	P88	Hås	Sweden	Pegmatite
Uraninite	P87	Hås	Sweden	Pegmatite
Uraninite	NRM-560070	Nilsby	Sweden	Pegmatite
Uraninite	NRM-571045:49	Stackebo	Sweden	Pegmatite
Uraninite	LAMNH-30222	Scotty mine, Oxford Co.	Maine, USA	Pegmatite*
Uraninite	UNM-337	Webb mine, Yancey Co.	North Carolina, USA	Pegmatitic veins in gneiss*
Galena	NRM-990118	Skatviken, Grythyttan	Sweden	Dolomite marble

*Uncertain, deduced from literature.

Uraninite crystal P88 was originally analysed by Welin and Blomqvist /1964/, and found to be concordant with an age of 930 Ma. This sample comes from a pegmatite at Hås, in SW Sweden. Other Swedish uraninite samples investigated in this study come from Stackebo (NRM-571045:49) and Nilsby (NRM-560070). These samples were found to be nearly concordant by Welin and Blomqvist /1964/ and come from ca 930 Ma old pegmatitic veins. Two promising uraninite crystals from USA were analysed in this study. The crystal LAMNH-30222 comes from Scotty mine, Oxford county, Maine, USA. The plutonic rocks of Western Maine, and related pegmatitic veins, are 380–325 Ma old /Lux and Guidotti, 1985/, indicating the age of the uraninite crystal. The sample UNM-337 from Webb mine, Yancey county, North Carolina, USA, come from an area of uranium occurrence in the Grandfather Mountain window. Uraninite from a pegmatite in Spruce Pine in the same area yielded U-Pb ages of 370–400 Ma /Davis et al., 1962/.

The galena sample NRM-990118 comes from Skatviken, Grythyttan, a locality in the Swedish ore district of Bergslagen. The sample consists of two galena crystals ca 3–4 mm in diameter, that come from a dolomite marble. Galena from Bergslagen is known for having a homogenous Pb isotopic composition /Sundblad, 1994/.

Selected grains (500 μm to 1mm) of uraninite were arranged in clusters on double-sided tape within moulds 25 mm in diameter and 25 mm thick. Epoxy resin was then poured in and allowed to harden. The hardened epoxy mounts were separated from the moulds and polished using 600–2400 grit sandpaper and 3μm–0.1μm diamond polishing compounds.

The samples were examined by reflected light microscopy as well as electron microscopy. Semi-quantitative chemical analyses were performed on carbon coated mounts under a scanning electron microscope fitted with an energy-dispersive X-ray analyzer (EDAX 9800). Sample P88 was analysed by IR reflectance spectroscopy to investigate the presence of water in the crystal.

2.2 EMPA (Electron Microprobe Analysis)

Chemical composition of uraninite LAMNH-30222 was determined by wavelength dispersive spectroscopy using an automated CAMECA 50 X-ray microanalyzer operated at 15 kV, a beam diameter of 10 μm, and counting times of 40 s per element. Synthetic UO_2 and minerals (grossular garnet for Si and Ca and galena for Pb) were used as standards. Detection limits were on the order of 0.1 wt%. The program PAP was used to reduce the data for the various elements. Oxygen contents of uraninite were calculated by stoichiometery assuming an ideal composition of UO_2.

Chemical composition of uraninite P88 was determined by wavelength dispersive spectroscopy (WDS) using a Cameca SX50 WDS at an operating voltage of 20kV, a beam current of 30 nA with a diameter of 2–10 μm. The counting time per element was set to 10–60 s or until 1% precision was attained. Background positions were analysed until half of the peak counts was reached. Data reduction was performed by ZAF corrections in the PAP program. Analytical standards were uraninite (U), vanadinite (Pb), wollastonite (Si, Ca), apatite (P), sphalerite (S), monazite (Th, La, Ce, Pr, Nd, Sm), hematite (Fe) and the pure elements for Y, Tb, Dy, Ho, Er. Oxygen was determined by stoichiometry. Detection limits were in the order of 0.15%.

2.3 TIMS

Thermal Ionisation Mass Spectrometry (TIMS) analyses were carried out on a Finnigan MAT 261 solid source mass spectrometer at the Laboratory for Isotope Geology, Swedish Museum of Natural History. The galena analysis was done by Joakim Mansfeld prior to the initiation of this study, using standard methods described in Holtstam and Mansfeld /2001/. Uraninite was analysed at three different times by Hans Schöberg, using the following method.

Micro samples of uraninite were collected by micro drilling or by pressing and grinding a sharp spike into the polished surface of the sample. The fragments and powders were weighed and dissolved in HNO_3. A mixed 233/235/208 spike was used for isotope dilution. The samples were purified and U and Pb isolated by anion exchange using 50μl AGI-x8 columns. Lead was analysed using silica gel on single Re filaments, and uranium was loaded in nitric acid on double Re-filaments.

$^{204}Pb/^{206}Pb$ is given as measured, other atomic ratios are corrected for mass discrimination, blank and initial Pb. The mass discrimination for Pb analyses was 0.18%/amu. Uranium mass discrimination (around 0.05%/amu) was calculated for each individual analysis using the double spike. Initial Pb correction was done according to Stacey and Kramers /1975/, using the composition of common Pb at the time of crystallisation.

Analytical precision of $^{207}Pb/^{206}Pb$ isotopic ratios is ca 0.05% (1σ), and on U/Pb ratios ca 0.1% (1σ). Data reduction and age calculation were done according to Ludwig /1991/, using the decay constants recommended by Steiger and Jäger /1977/.

2.4 SIMS

2.4.1 Introduction

SIMS analyses were performed with a Cameca IMS1270 at the NORDSIM facility, Sweden and with a Cameca IMS 4f at Oak Ridge National Laboratory, Tennessee. These ion microprobes differ in size, and therefore also in the mass resolution that can be achieved in practice. Mass resolution, i.e., the ability to separate ion beams of similar masses, is defined as the mass divided by the width of the base of the peak in mass units ($R = M/\Delta M_b$). The IMS 1270 has a larger turning radius and a larger secondary magnet than the IMS 4f, which leads to better transmission of secondary ions (i.e., higher sensitivity) at a high mass resolution ($R \approx 5000$). Hence, a large ion microprobe can be operated at a higher mass resolution than a small with a maintained high sensitivity.

During SIMS analyses, all the material, which is sputtered from the sample, forms a plasma above the sample surface. This plasma consists of both elemental and molecular ions, which can mutually interfere with the element of interest. These interferences can be dealt with by using high mass resolution or by high energy filtering. The high energy filtering technique is used when the mass resolution needed to resolve isobaric molecular interferences cannot be achieved /Hinton, 1995/. It is done by running the analysis at an accelerating voltage lower than the optimised. This causes ion yields to drop, because only ions of highest kinetic energy are extracted from the plasma. Due to the lower kinetic energy of the molecular ions relative to atomic ions, molecular interferences can be selectively removed by using the energy filtering technique.

During high mass resolution ion microprobe analyses, most interferences at heavy masses like Pb, can be resolved. However, to resolve Pb-hydrides such as $^{206}Pb^{1}H$ from ^{207}Pb requires a mass resolution of over 25 000, which is very difficult to obtain /Williams, 1998/. Hydrides have a similar energy distribution as atomic ions, and at high masses, hydrides cannot be removed by high energy filtering /Hinton, 1995/. Thus, hydride interferences are difficult to deal with in SIMS analyses.

The analytical conditions differed for NORDSIM and ORNL. Use of different analytical conditions, most notably energy filtering, can significantly influence the relationship between IMF and composition /e.g., Hervig et al.,1992/.

2.4.2 NORDSIM

The secondary ion accelerating voltage was 10 kV with the extraction electrode at -10 kV relative to the sample surface. A mass resolving power of about 5400 with an energy window of 30 eV was used to obtain flat top peaks. This mass resolution was sufficient to separate the REE-oxides from Pb. Ions were detected by an ETP electron multiplier coupled with an ion counting system with an overall deadtime of 25 ns. The primary current and details of the analytical set-up varied between sessions (Table 2-2).

Table 2-2. The analytical sessions during which the SIMS data were collected.

Session	Date	Sample	Comment
OR-1	03-jan-01	LAMNH30222	Pb:50V offset, 100nA, U: No offset, 5nA
		P88	Pb:50V offset, 30nA, U: 50V offset, 6nA
		NRM990118	50V offset: 50nA, No offset: 3 nA
OR-2	04-jan-01	LAMNH30222	Pb:50V offset, 85nA, U: No offset, 5nA
		P88	Pb:50V offset, 25nA, U: 50V offset, 6nA
		NRM990118	50V offset: 50nA
OR-3	05-jan-01	LAMNH30222	Pb:50V offset, 85nA, U: No offset, 4.5nA
		P88	Pb:50V offset, 30nA, U: 50V offset, 6nA
		NRM990118	50V offset: 50nA
1	15-sep-98	P88	Primary current: $3 \cdot 10^{-10}$A. Oxygen leak for calibration curve
2	16-sep-98	P88	Primary current: $3 \cdot 10^{-10}$A. Oxygen leak. Bad beam-shape. Paired data: two analyses after another in the same spot.
3	21-sep-98	P88	Primary current: $3 \cdot 10^{-10}$A. Two loose pieces in the sample holder pressed to the same level by a fingered spring. UO/UO measured.
4	22-sep-98	P88	Test U/U, UO/UO, UO_2/UO_2
5	23-sep-98	P88	Primary current $2 \cdot 10^{-11}$A.Two loose pieces, see above. UO/UO measured.
6	24-sep-98	P88	Primary current $1.2 \cdot 10^{-11}$A. Two loose pieces, see above. UO/UO measured.
7	20-mar-00	LAMNH30222	UO_2/UO_2, Primary current $1.4 \cdot 10^{-11}$A. Big strange background on the UO_2-peak.
8	21-mar-00	LAMNH30222	UO_2/UO_2, Primary current $1.5 \cdot 10^{-11}$A. Oxygen leak for calibration curve. Big strange background on the UO_2-peak.
9	22-mar-00	LAMNH30222	UO_2/UO_2, Primary current $1.5 \cdot 10^{-11}$A. Big strange background on the UO2-peak.
10	23-mar-00	LAMNH30222	UO_2/UO_2, Primary current $1.5 \cdot 10^{-11}$A. Oxygen leak for calibration curve construction. Unstable primary current.
11	07-jun-00	LAMNH30222	Primary current ca.1 nA
		NRM990118	Primary current $1 \cdot 10^{-10}$A
12	11-jun-00	LAMNH30222	Primary current ca 1 nA
		P88	Primary current $1 \cdot 10^{-10}$A
		NRM990118	Primary current $1 \cdot 10^{-10}$A
13	13-jun-00	LAMNH30222	Primary current $5 \cdot 10^{-10}$A. Primary slightly unstable.
		P88	Primary current $2 \cdot 10^{-10}$A.
		NRM990118	Primary current $1 \cdot 10^{-10}$A
14	03-nov-00	LAMNH30222	First session after power failure. Warm room. Primary current $6 \cdot 10^{-10}$A Unstable Pb counts.
		P88	Primary current $4 \cdot 10^{-10}$A. Unstable Pb counts
15	07-nov-00	LAMNH30222	Primary current ca 1 nA. Unstable Pb counts
16	22-jan-01	LAMNH30222	3 points. ca 1 nA. 5 · 3 cycles
		P88	3 points ca 0.5 nA. 5 · 3 cycles
17	23-jan-01	LAMNH30222	Cold Trap. 6 points. ca 1 nA
		P88	Cold Trap. 5 points. ca 0.5 nA
18a	24-jan-01	LAMNH30222	50V offset. 7 points. ca 4 nA 5 · 4 cycles
		P88	50V offset. 7 points. ca 1nA
18b	24-jan-01	LAMNH30222	No offset. 3 points. ca 1nA
		P88	No offset. 3 points. ca 0.5nA
19	12-feb-01	LAMNH30222	After vacuum. ca 0.1nA, small exit slit. 6 points. U-oxides+H
		P88	After vacuum. 0.7-0.6 nA, small exit slit. 6 points. U-oxides+H
20	12-feb-01	LAMNH30222	50V offset. After vacuum, 2nA. 5 points. U-oxides+H
		P88	50V offset. After vacuum, 4 points, 2nA. U-oxides+H

In general, a 0.1–1 nA primary ion beam of O_2^- was focused to a 15 · 30 µm spot using a 100 µm aperture in the primary column. When energy offset was used, the primary current was 1–4 nA. High resolution mass scans indicate that all isobaric interferences (apart from hydrides) were fully resolved. In general, an analysis lasted 10–20 minutes comprising 10–30 analysis cycles. During uraninite analyses, the following species were detected sequentially by switching the magnetic field:

Sessions 1–2: $^{04}Pb^+$, 204.2 (background), $^{206}Pb^+$, $^{207}Pb^+$, $^{208}Pb^+$, $^{235}U^+$, $^{238}U^+$, $^{232}Th^{16}O^+$, $^{238}U^{16}O^+$. (12 cycles, 10 minutes).

Sessions 3, 5–6: $^{204}Pb^+$, 204.2 (background), $^{206}Pb^+$, $^{207}Pb^+$, $^{208}Pb^+$, $^{238}U^+$, $^{232}Th^{16}O^+$, $^{235}U^{16}O^+$, $^{238}U^{16}O^+$. (12 cycles, 10–15 minutes).

Session 4: $^{204}Pb^+$, 204.2 (background), $^{206}Pb^+$, $^{207}Pb^+$, $^{208}Pb^+$, $^{235}U^+$, $^{238}U^+$, $^{232}Th^{16}O^+$, $^{235}U^{16}O^+$, $^{238}U^{16}O^+$, $^{235}U^{16}O_2^+$, $^{238}U^{16}O_2^+$. (12 cycles, 15 minutes).

Sessions 7–10: $^{04}Pb^+$, 204.2 (background), $^{206}Pb^+$, $^{207}Pb^+$, $^{208}Pb^+$, $^{238}U^+$, $^{238}U^{16}O^+$, $^{235}U^{16}O_2^+$, $^{238}U^{16}O_2^+$. (8 cycles, 10 minutes).

Sessions 11–13: ^{197}Au, $^{204}Pb^+$, $^{206}Pb^+$, $^{207}Pb^+$, $^{208}Pb^+$, $^{235}U^+$, $^{238}U^+$. (30 cycles, 20 minutes).

Sessions 14–15: $^{04}Pb^+$, $^{206}Pb^+$, $^{207}Pb^+$, $^{208}Pb^+$, $^{235}U^+$, $^{238}U^+$. (30 cycles, 20 minutes).

Sessions 16–18b: 200 (dummy) , $^{204}Pb^+$, $^{206}Pb^+$, $^{207}Pb^+$, $^{208}Pb^+$, 209 ($^{209}Bi^+$ and/or $^{208}Pb^1H^+$), $^{235}U^+$, $^{238}U^+$, $^{238}U^1H^+$. (15 cycles, 15 minutes). A liquid nitrogen cold trap was used during session 17, and 50 V energy offset was used during session 18a.

Sessions 19–20: 202 (dummy), $^{204}Pb^+$, $^{206}Pb^+$, $^{207}Pb^+$, $^{208}Pb^+$, 209 ($^{209}Bi^+$ and/or $^{208}Pb^1H^+$), $^{235}U^+$, $^{238}U^+$, $^{238}U^1H^+$, $^{235}U^{16}O^+$, $^{235}U^{16}O^1H^+$, $^{238}U^{16}O^+$, $^{238}U^{16}O^1H^+$. (15 cycles, 20 minutes.) The sample was held in vacuum of ca 0.3 mbar for 5 days before analysis. The air outside the dessicator was heated to ca 50°C. During session 20 a 50 V energy offset was used.

During galena analyses, only the elemental Pb isotopes were measured. A galena analysis lasted 10 minutes comprising 40 analysis cycles.

2.4.3 Oak Ridge National Laboratory

U and Pb isotopic analysis were also obtained using the small radius Cameca IMS 4f ion microprobe at Oak Ridge National Laboratory (Table 2-2). In general, the secondary ion accelerating voltage was 4.5 kV with the extraction electrode at –4.5 kV relative to the sample surface. A mass resolving power of about 400 with an energy window of ±20 eV was used to obtain flat top peaks. The mass resolution was not sufficient to resolve oxide and hydride interferences; therefore, Pb isotopes were analysed using an energy offset of –50 V, which suppressed the molecular interferences. A liquid nitrogen cold trap was used to minimise hydride interferences. Since there are fewer interferences associated with the isotopes of U, the U isotopes were subsequently analysed using a 0 V energy offset from the same spot. When an energy offset was used to suppress interferences (e.g., for Pb analyses) a 30–85 nA primary ion beam of O^- was focused to a 15 · 30 µm spot using a 100 µm aperture in the primary column. However,

when no offset was required (e.g., U isotope analyses) a 3 to 6nA primary beam was used.

Ions were detected by a Balzers electron multiplier coupled with an ion counting system with an overall deadtime of 15 ns. For Pb isotopic analysis, the following species were detected sequentially by switching the magnetic field: 203.5 (background), $^{204}Pb^{+}$, $^{206}Pb^{+}$, $^{207}Pb^{+}$, $^{208}Pb^{+}$, 209 ($^{209}Bi^{+}$ and/or $^{208}Pb^{1}H^{+}$). A typical Pb analysis lasted ca 6 minutes and comprised 10 analysis cycles. For uraninite, this was followed by the U isotopic analysis, during which the following species were detected: $^{235}U^{+}$, $^{238}U^{+}$, $^{238}U^{1}H^{+}$. A typical U analysis lasted ca 2 minutes and comprised 20 analysis cycles.

3 Results

3.1 Sample petrography and EMPA

3.1.1 Swedish uraninite: P88, P87, NRM-560070 and NRM-571045:49

The polished fragments of Swedish uraninite crystals reveal veins, cracks and inclusions in the optical microscope. EDS (Energy Dispersive Spectroscopy) analyses of the inclusions and veins show that these are U and Pb rich and contain a substantial amount of Si, Ca and Fe. These features are shared by all samples from the Swedish localities. There are well preserved parts of unaltered uraninite between the veins and fractures.

The polished surface of uraninite crystal P88 is ca 2 · 6 mm. Examinations by optical and electron microscopy (EDS) revealed the existence of fractures and veins which contain mainly U, Pb and Si. There are also micro inclusions of galena. Chemical analyses by wavelength dispersive spectroscopy (WDS) show that the crystals contain (in wt%): 71.5% UO_2, 10.2% PbO, 4.4% ThO_2, 3.1% Y_2O_3, 0.70% Ca, 0.18% SiO_2 and ca 2.7% REE-oxides (detected elements: Nd, (Sm), Gd, Dy, Er and Yb). Using reflectance IR spectroscopy, no water (OH or H_2O) could be detected in P88. This indicates that the water content is lower than 1 wt%.

3.1.2 American uraninite: LAMNH-30222 and UNM-337

These samples are single uraninite crystals. LAMNH-30222 is ca 1.5 · 1.5 mm (polished sample in epoxy). Microscope studies (optical and SEM) of LAMNH-30222 reveal small inclusions of galena and chalcopyrite, and some Mg-Mn-bearing phase. Electron microprobe analyses of LAMNH-30222 show that the crystal contains 92.4 wt% UO_2, 4.7 wt% PbO and 0.04 wt% FeO. UNM-337 is a large crystal, ca 1 cm, from which a piece was taken. The size of the polished surface is 5 · 3 mm, and it contains small Si- and Fe-rich inclusions.

3.1.3 Galena NRM-990118

No EDS or EMPA data exists for the galena sample.

3.2 TIMS results

Results of the TIMS analyses are summarised in Table 3-1. The composition of the galena sample (NRM-990118) is found to be in agreement with previous analyses of galena from Bergslagen /Sundblad, 1994/. Considering the homogenous character of Pb isotopic composition of galena from Bergslagen, this sample was used as a preliminary standard for SIMS analyses. The uraninite U-Pb data is plotted on a concordia diagram

Table 3-1. Isotopic compositions of the investigated samples measured with TIMS.

Sample number	TIMS sample	weight (mg)	206/204	207/206	208/206	207/235	206/238	Age6/38	Age7/35	Age7/6
P88	P88	0.0023	50000	0.06919	0.02049	1.421	0.149	895	898	905
P87	P87-2	0.0023	29000	0.06963	0.01850	1.399	0.146	877	889	917
NRM-560070	N-10	0.0035	>50000	0.07040	0.02442	1.469	0.151	908	918	941
NRM-571045:49	S-8	0.0028	15000	0.07177	0.00593	1.435	0.145	873	904	980
LAMNH-30222	MF-1a	0.002	4200	0.05388	0.00254	0.409	0.055	346	348	365
LAMNH-30222	MF-3	0.0036	>50000	0.05377	0.00264	0.411	0.055	348	350	362
LAMNH-30222	MF-3a	0.0155	>50000	0.05377	0.00264	0.411	0.056	349	351	363
UNM-337	UNM-2	0.0032	>50000	0.05472	0.00979	0.445	0.059	370	374	400
UNM-337	UNM-2a	0.0051	>50000	0.05424	0.00095	0.426	0.057	356	360	383
NRM-990118			15.74	0.976	2.241					

in Figure 3-1. Figures 3-2, 3-3, and 3-4 show close-ups of the data, which are plotted with 2σ error ellipses. Based on these results, sample P88 and LAMNH-30222 were chosen for further analyses by SIMS. Sample P88, the first uraninite crystal to be analysed (in 1998) yielded an age of ca 900 Ma, but is on the verge of being discordant (Figure 3-3). Three analyses of sample LAMNH-30222 yielded similar ages of ca 350 Ma (Figure 3-2). These two potentially good ion microprobe uraninite standards are concordant or nearly concordant and have much different ages and radiogenic Pb contents.

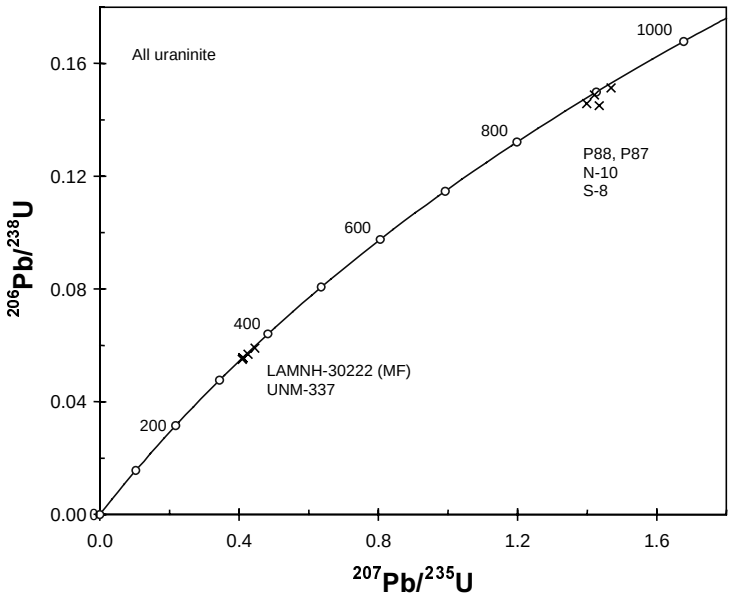

Figure 3-1*. All TIMS U-Pb data of uraninite.*

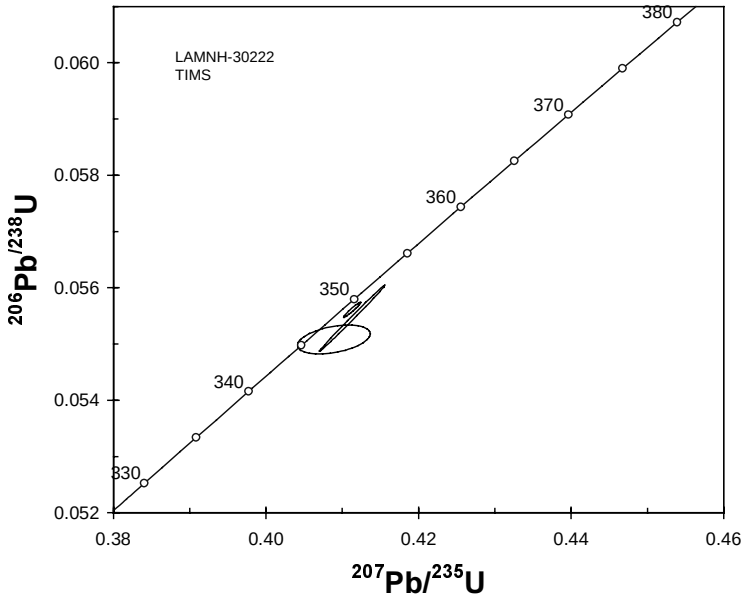

Figure 3-2. *TIMS U-Pb data of LAMNH-30222. 2σ error ellipses.*

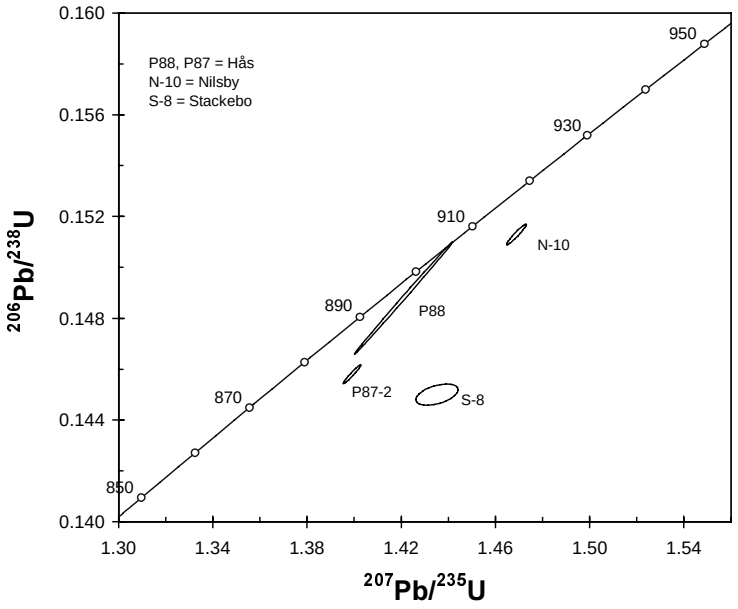

Figure 3-3. *TIMS U-Pb data of uraninite from Swedish pegmatites. 2σ error ellipses.*

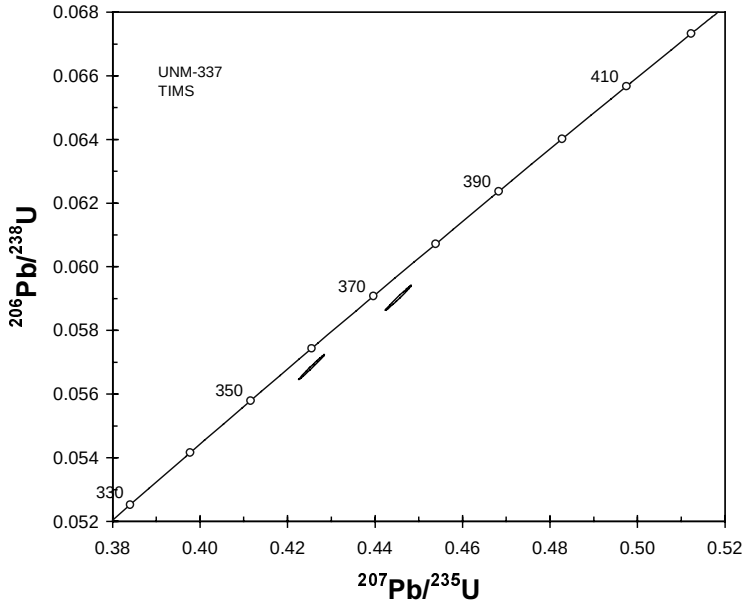

Figure 3-4. *TIMS U-Pb data of uraninite UNM-337. 2σ error ellipses.*

3.3 SIMS results

3.3.1 Introduction

The experiments were carried out during several analytical sessions from 1998 to 2001 (Table 2-2; Appendix). However, poor reproducibility encountered during some analytical sessions (Table 3-2) precluded their use in the final fractionation factor calculations. In general, we have only considered sessions where the standard deviation (σ) is at maximum three times larger than the average error of individual analyses. Analytical sessions where 1σ is greater than 1% are not considered. The reasons for poor reproducibility during sessions 3–6, 7–10 and 14–15, were found to be related to sample geometry and secondary magnet hysteresis.

3.3.2 Galena

Galena was analysed during sessions OR-1, OR-2 and OR-3 at ORNL and sessions 11,12 and 13 at the NORDSIM facility (Table 2-2; Table A-1 Appendix). In general, galena shows very stable and reproducible results. A significant difference between the SIMS measured ratios and the TIMS values is observed. The fractionation factors for the Pb isotopes are calculated by taking the isotopic ratios measured by TIMS and dividing them by the average of the ratios for each SIMS session (Table 3-3; Figure 3-5).

An inter-laboratory comparison shows that the fractionation, in favour of the lighter isotope of Pb, is close to the same at both facilities (see Figure 3-5). At NORDSIM, the average fractionation factor is 0.46±0.01%/amu (1σ), while the ORNL the average fractionation factor is slightly higher (0.56±0.04%/amu (1σ)).

Table 3-2. Performance during analytical sessions, based on $^{207}Pb/^{206}Pb$ measurements. Original data for every session is found in the Appendix. St.Dev = Standard Deviation, Av. Err = Average Error of individual analyses.

Session	Sample	1 Standard Deviation (%)	Average Error (1σ)%	Std.Dev/ Av.Err
OR-1	P88	0.11	0.08	1.51
	LAMNH	0.19	0.11	1.65
	NRM990118	0.09	0.06	1.33
OR-2	P88	0.08	0.13	0.60
	LAMNH	0.19	0.16	1.15
	NRM990118	0.06	0.08	0.80
OR-3	P88	0.13	0.14	0.96
	LAMNH	0.12	0.21	0.58
	NRM990118	0.06	0.11	0.58
1	P88	0.34	0.17	1.95
2	P88	0.28	0.15	1.80
3	P88	1.06	0.19	5.72
4	P88	0.35	0.11	3.17
5	P88	7.95	0.95	8.40
6	P88	3.03	1.18	2.57
7	LAMNH	1.65	0.49	3.35
8	LAMNH	1.55	0.58	2.70
9	LAMNH	1.25	0.64	1.95
10	LAMNH	1.33	0.47	2.81
11	LAMNH	0.41	0.23	1.75
	NRM990118	0.33	0.23	1.45
12	P88	0.39	0.18	2.16
	LAMNH	0.45	0.35	1.28
	NRM990118	0.22	0.22	1.00
13	P88	0.33	0.11	2.89
	LAMNH	0.27	0.28	0.96
	NRM990118	0.38	0.21	1.81
14	P88	2.48	0.29	8.47
	LAMNH	3.74	0.29	12.74
15	LAMNH	2.03	0.30	6.70
16	P88	0.14	0.13	1.12
	LAMNH	0.87	0.20	4.43
17	P88	0.12	0.11	1.10
	LAMNH	0.33	0.30	1.12
18a	P88	0.56	0.36	1.55
	LAMNH	0.78	0.74	1.05
18b	P88	0.12	0.12	0.99
	LAMNH	0.07	0.30	0.24
19	P88	0.16	0.12	1.30
	LAMNH	0.34	0.28	1.22
20	P88	0.35	0.31	1.14
	LAMNH	0.45	0.38	1.18

Table 3-3. Calculation of fractionation factors for Pb in galena. Errors are given as 1σ. FF= Fractionation factor.

Session	Average	±	Err(%)	TIMS	±	FF	±	Fractionation/ amu%	±
$^{206}Pb/^{204}Pb$									
OR-1	15.519	0.0231	0.15	15.736	0.011	1.014	0.002	0.70	0.08
OR-2	15.526	0.0168	0.11	15.736	0.011	1.014	0.001	0.68	0.06
OR-3	15.539	0.0381	0.25	15.736	0.011	1.013	0.003	0.63	0.13
11	15.600	0.0476	0.31	15.736	0.011	1.009	0.003	0.44	0.16
12	15.586	0.0293	0.19	15.736	0.011	1.010	0.002	0.48	0.10
13	15.567	0.0293	0.19	15.736	0.011	1.011	0.002	0.54	0.10
$^{207}Pb/^{206}Pb$									
OR-1	0.971	0.0008	0.09	0.976	0.002	1.005	0.002	0.50	0.20
OR-2	0.972	0.0006	0.06	0.976	0.002	1.004	0.002	0.42	0.20
OR-3	0.972	0.0006	0.06	0.976	0.002	1.004	0.002	0.38	0.19
11	0.971	0.0032	0.33	0.976	0.002	1.005	0.004	0.48	0.38
12	0.972	0.0021	0.22	0.976	0.002	1.004	0.003	0.45	0.29
13	0.972	0.0037	0.38	0.976	0.002	1.004	0.004	0.44	0.43
$^{208}Pb/^{206}Pb$									
OR-1	2.213	0.0023	0.10	2.241	0.005	1.013	0.002	0.63	0.12
OR-2	2.219	0.0042	0.19	2.241	0.005	1.010	0.003	0.50	0.15
OR-3	2.214	0.0015	0.07	2.241	0.005	1.012	0.002	0.60	0.12
11	2.221	0.0025	0.11	2.241	0.005	1.009	0.003	0.45	0.13
12	2.221	0.0024	0.11	2.241	0.005	1.009	0.002	0.44	0.12
13	2.221	0.0024	0.11	2.241	0.005	1.009	0.002	0.45	0.12

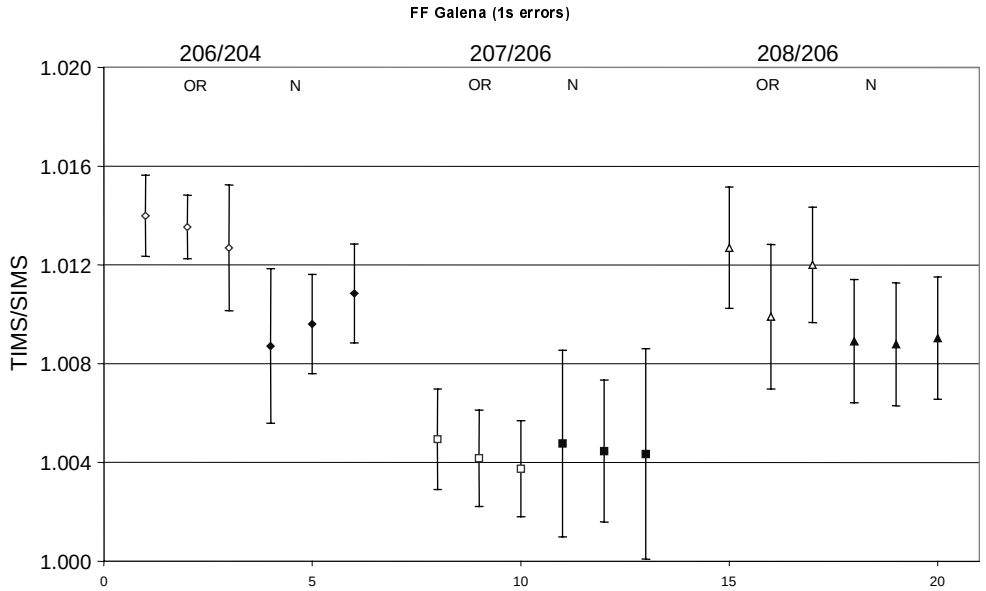

Figure 3-5. *Fractionation factors (FF=TIMS/SIMS) for Pb isotopes in galena measured during sessions OR-1, OR-2, OR-3 (white symbols) and 11, 12 13 (filled symbols). Diamonds= $^{206}Pb/^{204}Pb$, squares = $^{207}Pb/^{206}Pb$, triangles = $^{208}Pb/^{206}Pb$. OR = Oak Ridge, N = Nordsim.*

3.3.3 Uraninite

The mass spectra of the two uraninite samples are shown in Figure 3-6. The spectrum of P88 uraninite shows that there are interferences associated with each Pb mass as well as two peaks at mass 209. The interferences are most likely REE oxides (YbO_2, GdO_3, LuO_2, DyO_3), which are found by electron microprobe in P88 but not in LAMNH-30222. At mass 209, one of the peaks may be $^{208}Pb^{1}H$, which is irresolvable from ^{209}Bi. Although Bi was not detected by the electron microprobe in either of the two uraninite samples, the ion microprobe has a lower detection limit than the electron microprobe, and a small amount of Bi may still be present in the sample. The other peak at mass 209 in the P88 mass spectrum may be either $^{161}Dy^{16}O_3$ or $^{145}Nd^{16}O_4$. The spectrum for LAMNH-30222 shows no interferences on the Pb peaks, but also a peak at mass 209. This peak is likely ^{209}Bi or $^{208}Pb^{1}H$.

The spectra for the U isotopes are less complex. Hydride peaks occur at masses 239 ($^{238}U^{1}H$) and 255 ($^{238}U^{16}O^{1}H$), which clearly shows the presence of hydrides. Hydride interferences with ^{235}U such as $^{234}U^{1}H$ are negligible. Possible interferences with ^{238}U are mainly $^{206}Pb^{16}O_2$ and $^{206}Pb^{32}S$. However, these molecular interferences are likely negligible because of their low abundances relative to the U isotopes.

Figure 3-7 shows the intensity of the energy spectra of a number of ions at different energy offsets. U isotopes have a much broader energy distribution than the Pb isotopes. Mass 239 has basically the same energy distribution as the U isotopes, a behaviour expected of $^{238}U^{1}H$ /Hinton 1995/. Mass 204, found in sample P88, is a molecular interference (REE-oxide), which can be seen by the narrow energy distribution.

U and Pb data of uraninite collected during SIMS analytical sessions are reported in Appendix (Table A-2 and A-3). Due to the small amount of material that is sputtered, ^{204}Pb peak is virtually non-detectable. Therefore, the amount of common lead is negligible and correction is not necessary for the majority of uraninite analyses. However, when ^{204}Pb was detected, common Pb correction has been performed and where an effect has been significant, the corrected value has been used. The composition of the common Pb was chosen according to Stacey and Kramers /1975/ at the time of uraninite crystallisation, i.e. 900 Ma for P88 and 350 Ma for LAMNH-30222.

The fractionation factors for Pb isotopic analysis of uraninite are calculated from the average of each SIMS analytical session (Table 3-4; Figure 3-8). The data obtained at ORNL indicates that the fractionation of Pb isotopes is approximately zero. This result differs from most of the NORDSIM sessions. The average of the NORDSIM sessions (excluding 17, 18a, 19 and 20) is approximately 1%/amu in favour of the heavier Pb isotope. This number becomes smaller during those NORDSIM sessions when some efforts were made to mimic the ORNL analytical conditions, e.g., use a cold trap (session 17), running with a 50 V offset (sessions 18a and 20) and letting the sample dry out in vacuum for some days before analyses (sessions 19 and 20). A 50 V offset appear to have the most significant effect. The average fractionation during these NORDSIM sessions is ca 0.4%/amu, in favour of the heavier isotope.

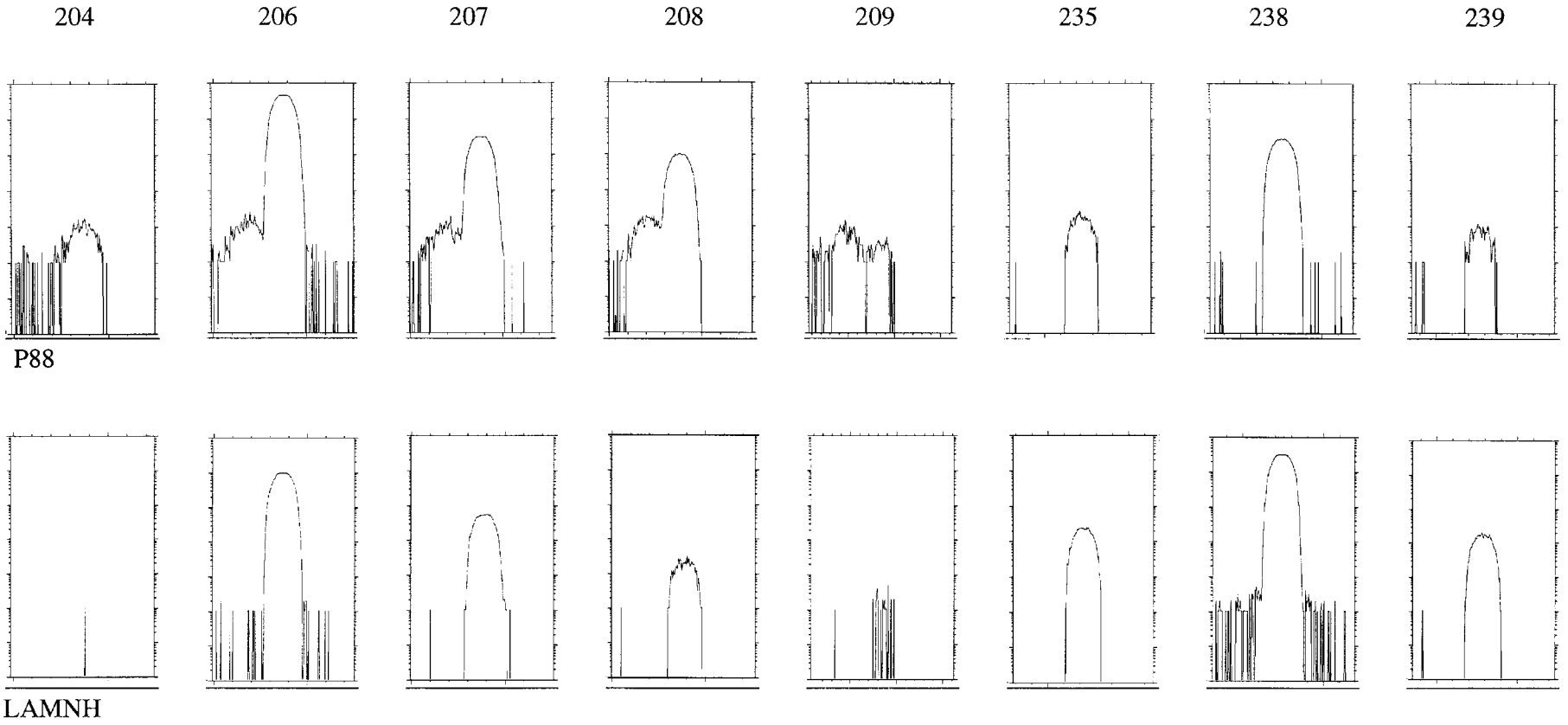

Figure 3-6. *Mass spectra for uraninite P88 and LAMNH measured at NORDSIM.Y-axis is logarithmic from 10^{-1} to 10^{6} counts/second. The width of each window is 0.15 amu. Mass resolution was set at ca. 5400. Primary current for P88 was $5 \cdot 10^{-10}$A, for LAMNH $1 \cdot 10^{-9}$A.*

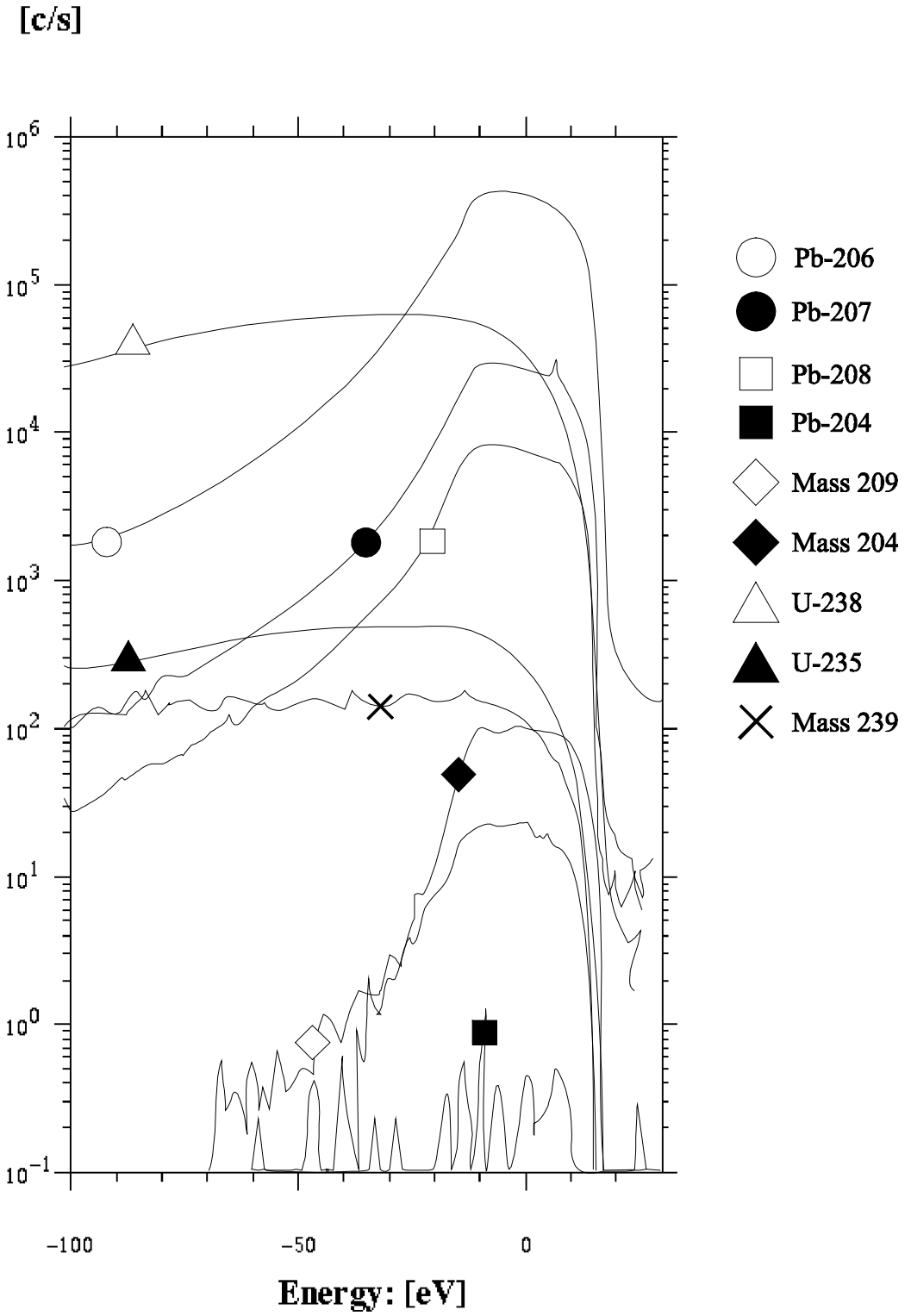

Figure 3-7. *Energy spectra of ion species in uraninite P88 during SIMS analyses (Cameca 1270).*

Table 3-4. Calculation of fractionation factors for Pb isotopes in uraninite. Errors are given as 1σ. FF = Fractionation factor

Session	Sample	Average $^{207}Pb/^{206}Pb$	Err (%)	TIMS	Err (%)	FF	±	Fractionation/ amu (%)	±
OR-1	P88	0.0693	0.11	0.0692	0.04	0.9982	0.001	0.18	0.12
	LAMNH	0.0537	0.19	0.0538	0.12	1.0015	0.002	-0.15	0.22
OR-2	P88	0.0694	0.08	0.0692	0.04	0.9973	0.001	0.27	0.09
	LAMNH	0.0538	0.19	0.0538	0.12	0.9994	0.002	0.06	0.22
OR-3	P88	0.0694	0.13	0.0692	0.04	0.9965	0.001	0.35	0.14
	LAMNH	0.0536	0.12	0.0538	0.12	1.0033	0.002	-0.33	0.17
1	P88	0.0698	0.34	0.0692	0.04	0.9910	0.003	0.90	0.34
2	P88	0.0697	0.28	0.0692	0.04	0.9932	0.003	0.68	0.28
11	LAMNH	0.0545	0.41	0.0538	0.12	0.9877	0.004	1.23	0.42
12	P88	0.0698	0.39	0.0692	0.04	0.9920	0.004	0.80	0.39
	LAMNH	0.0543	0.45	0.0538	0.12	0.9905	0.005	0.95	0.46
13	P88	0.0706	0.33	0.0692	0.04	0.9794	0.003	2.06	0.33
	LAMNH	0.0551	0.27	0.0538	0.12	0.9768	0.003	2.32	0.29
16	P88	0.0696	0.14	0.0692	0.04	0.9946	0.001	0.54	0.15
	LAMNH	0.0544	0.87	0.0538	0.12	0.9889	0.009	1.11	0.87
17	P88	0.0695	0.12	0.0692	0.04	0.9960	0.001	0.40	0.13
	LAMNH	0.0543	0.33	0.0538	0.12	0.9903	0.003	0.97	0.35
18a	P88	0.0693	0.56	0.0692	0.04	0.9988	0.006	0.12	0.56
	LAMNH	0.0540	0.78	0.0538	0.12	0.9964	0.008	0.36	0.79
18b	P88	0.0696	0.12	0.0692	0.04	0.9947	0.001	0.53	0.13
	LAMNH	0.0546	0.07	0.0538	0.12	0.9855	0.001	1.45	0.14
19	P88	0.0694	0.16	0.0692	0.04	0.9976	0.002	0.24	0.16
	LAMNH	0.0540	0.34	0.0538	0.12	0.9966	0.004	0.34	0.36
20	P88	0.0694	0.35	0.0692	0.04	0.9970	0.004	0.30	0.35
	LAMNH	0.0539	0.45	0.0538	0.12	0.9984	0.005	0.16	0.46

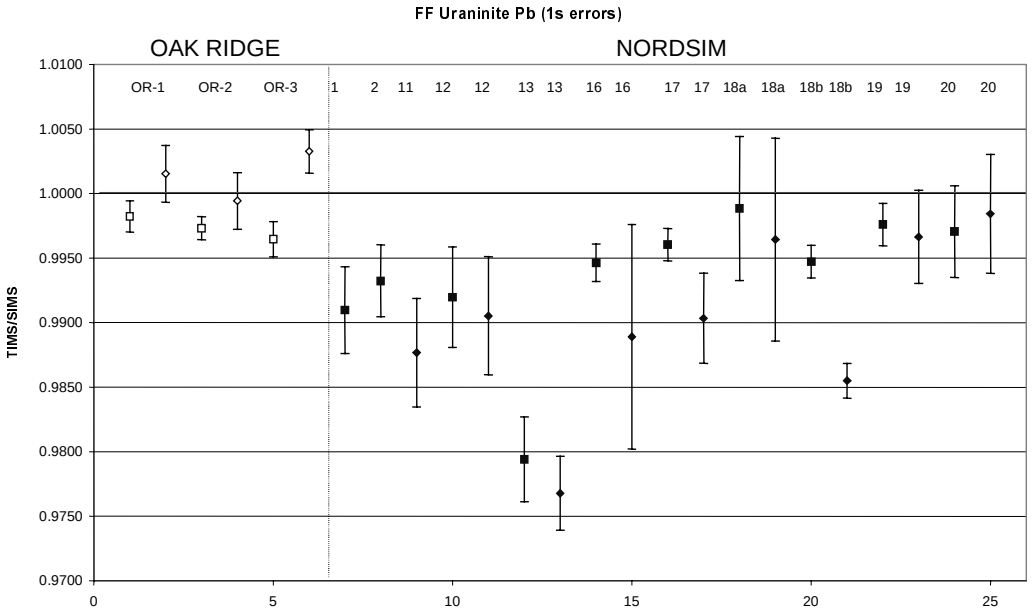

Figure 3-8. *Fractionation factors (FF=TIMS/SIMS) for uraninite $^{207}Pb/^{206}Pb$ measured at Oak Ridge (white symbols) and Nordsim (filled symbols). Squares = P88, diamonds = LAMNH. The session number is indicated above the data in the upper part of the diagram.*

The fractionation factors for U isotopic analysis of uraninite are calculated by dividing the average of each SIMS analytical session with the accepted ratio for $^{235}U/^{238}U$ (0.00725) (Table 3-5; Figure 3-9). The fractionation factor for U isotopes calculated from data collected at ORNL and NORDSIM is 1.4±0.1%/amu (1σ) and 1.4±0.4%/amu, respectively. Thus, the fractionation of U isotopes is determined to ca 1.4%/amu in favour of the lighter isotope. However, some analytical sessions deviate from this value. For example, a fractionation factor calculated from data collected during session 13 deviates from the 1.4%/amu value, probably due to duoplasmatron instability. During session 18a, a 50 V offset was used, which resulted in only a minor change in the mass bias (Figure 3-9).

Table 3-5. Calculation of fractionation factors for U in uraninite. Errors are given as 1σ. FF = Fractionation Factor.

Sessions	Sample	Average $^{235}U/^{238}U$	Err (%)	NATURAL	FF	±	Fractionation/ amu%	±
OR-1	P88	0.00760	0.56	0.00725	0.9540	0.005	1.53	0.18
	LAMNH	0.00755	0.43	0.00725	0.9605	0.004	1.32	0.14
OR-2	P88	0.00759	0.37	0.00725	0.9558	0.004	1.47	0.12
	LAMNH	0.00760	0.81	0.00725	0.9542	0.008	1.53	0.26
OR-3	P88	0.00761	0.62	0.00725	0.9533	0.006	1.56	0.20
	LAMNH	0.00753	0.45	0.00725	0.9627	0.004	1.24	0.14
1	P88	0.00765	0.94	0.00725	0.9483	0.009	1.72	0.30
2	P88	0.00765	1.54	0.00725	0.9483	0.015	1.72	0.49
11	LA	0.00748	0.73	0.00725	0.9694	0.007	1.02	0.23
12	P88	0.00762	1.32	0.00725	0.9521	0.013	1.60	0.42
	LA	0.00747	0.53	0.00725	0.9705	0.005	0.98	0.17
13	P88	0.00762	0.57	0.00725	0.9512	0.005	1.63	0.18
	LA	0.00788	0.96	0.00725	0.9197	0.009	2.68	0.29
16	P88	0.00758	0.35	0.00725	0.9565	0.003	1.45	0.11
	LA	0.00752	0.24	0.00725	0.9643	0.002	1.19	0.08
17	P88	0.00754	0.57	0.00725	0.9614	0.005	1.29	0.18
	LA	0.00753	0.15	0.00725	0.9629	0.001	1.24	0.05
18a	P88	0.00752	0.25	0.00725	0.9644	0.002	1.19	0.08
	LA	0.00745	0.20	0.00725	0.9729	0.002	0.90	0.06
18b	P88	0.00757	0.65	0.00725	0.9581	0.006	1.40	0.21
	LA	0.00753	0.24	0.00725	0.9633	0.002	1.22	0.08
19	P88	0.00756	0.26	0.00725	0.9587	0.003	1.38	0.08
	LA	0.00757	0.33	0.00725	0.9574	0.003	1.42	0.10
20	P88	0.00752	0.25	0.00725	0.9646	0.002	1.18	0.08
	LA	0.00750	0.16	0.00725	0.9662	0.002	1.13	0.05

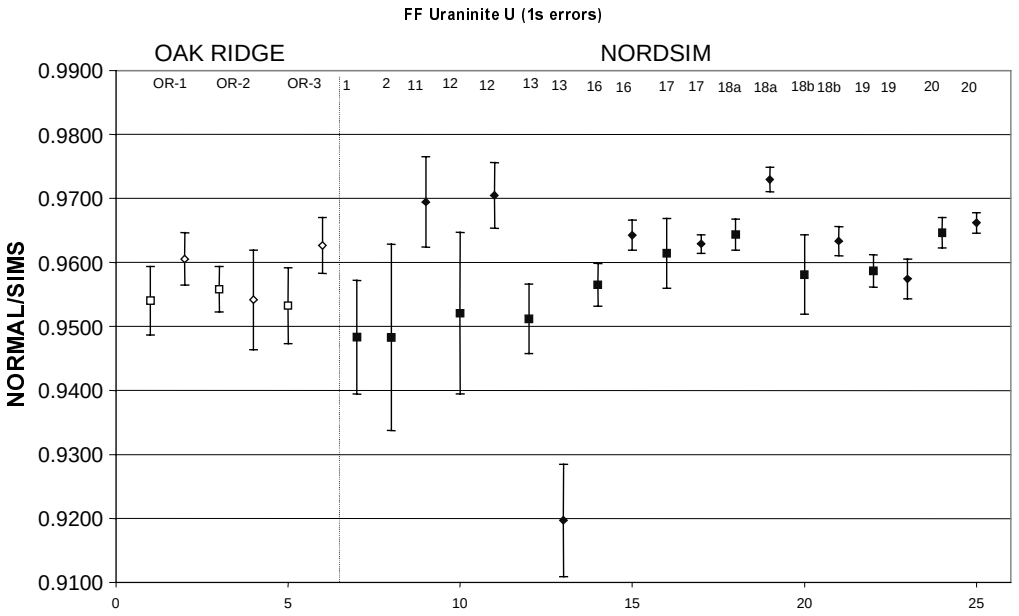

Figure 3-9. *Fractionation factors (FF=TIMS/SIMS) for uraninite $^{207}Pb/^{206}Pb$ measured at Oak Ridge(white symbols) and Nordsim (filled symbols). Squares = P88, diamonds = LAMNH. The session number is indicated above the data in the upper part of the diagram.*

Possible hydride interferences with the Pb and U isotopes were monitored during analytical sessions OR-1, OR-2, OR-3 at ORNL, and sessions 16 to 20 at NORDSIM (Table 3-6; Figure 3-10; Table A-4 Appendix), by measuring the assumed hydride peaks at 209 and 239. The average of measured ratios between mass 209 and ^{206}Pb in each session have been compared. The amount of measured mass 209 is basically the same in every session. This is true for both uraninite crystals. The amount of measured mass 239 does, however, change significantly between sessions for both uraninite crystals. Least amount of 239 was measured during the ORNL sessions and the NORDSIM sessions where 50 V offset where used (18a and 20). These sessions are also the sessions with smallest apparent fractionation of Pb isotopes, which indicates a correlation between the measured amounts of uranium hydrides and the apparent fractionation of Pb isotopes. This correlation has been further illustrated in Figure 3-11.

Table 3-6. Averages of hydride measurements (209/206 and 239/238) in uraninite. Errors are given as 1σ.

Session	Sample	209/206	±	239/238	±	Sample	209/206	±	239/238	±
OR-1	P88	0.00008	0.00000	0.00080	0.00023	LAMNH	0.00009	0.00005	0.00181	0.00010
OR-2	P88	0.00008	0.00000	0.00088	0.00004	LAMNH	0.00019	0.00004	0.00178	0.00024
OR-3	P88	0.00008	0.00001	0.00082	0.00008	LAMNH	0.00015	0.00007	0.00182	0.00009
16	P88	0.00007	0.00000	0.00267	0.00039	LAMNH	0.00009	0.00006	0.00424	0.00050
17	P88	0.00007	0.00000	0.00156	0.00013	LAMNH	0.00010	0.00004	0.00304	0.00006
18a	P88	0.00006	0.00001	0.00116	0.00009	LAMNH	0.00005	0.00002	0.00175	0.00012
18b	P88	0.00007	0.00000	0.00171	0.00010	LAMNH	0.00008	0.00001	0.00378	0.00021
19	P88	0.00006	0.00000	0.00133	0.00011	LAMNH	0.00012	0.00007	0.00218	0.00018
20	P88	0.00005	0.00000	0.00094	0.00002	LAMNH	0.00004	0.00002	0.00107	0.00009

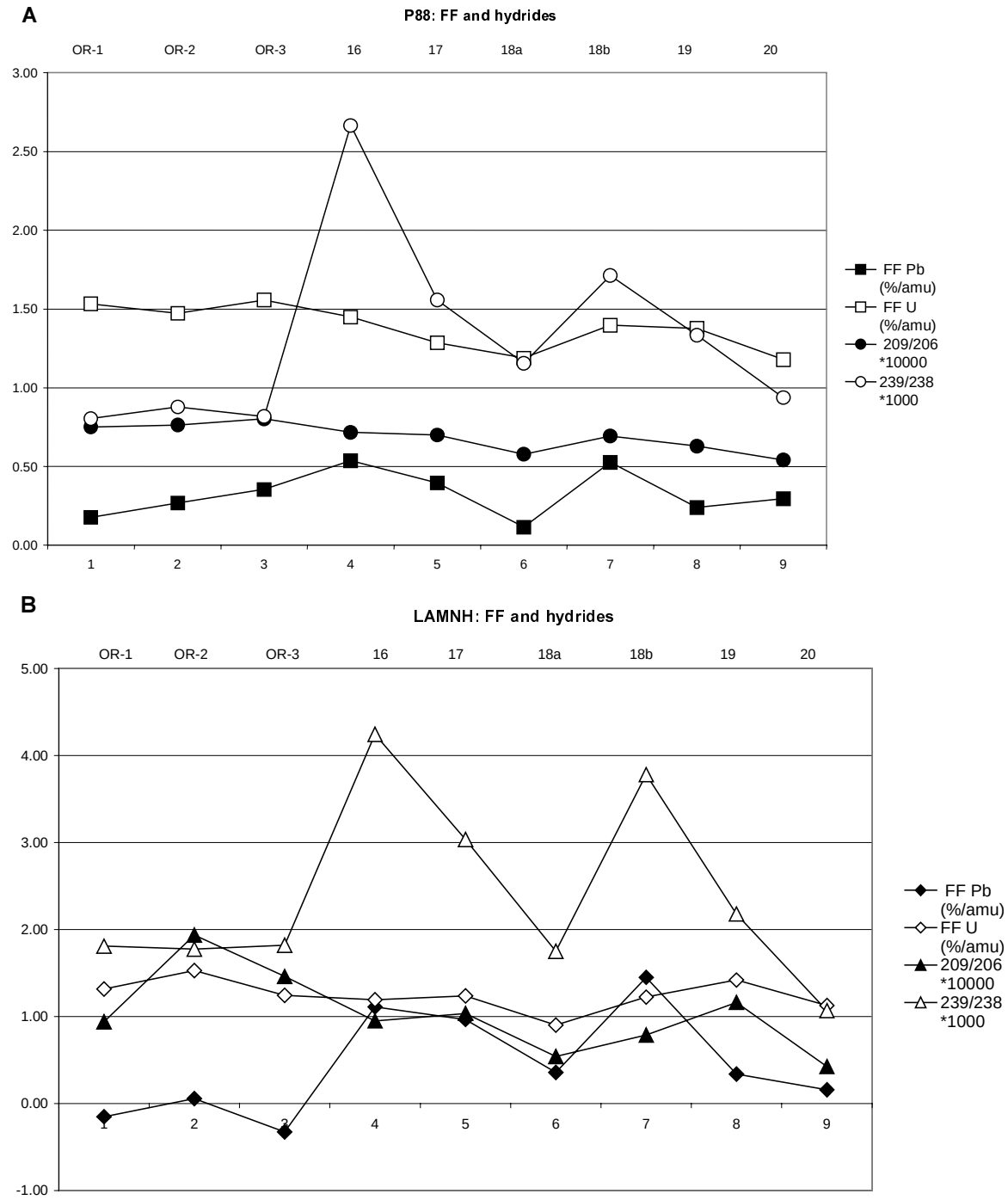

***Figure 3-10. A**, P88 **B**, LAMNH. The measured amount of mass 209 and 239, given as $209/206 \cdot 10^4$ and $239/238 \cdot 10^3$. Averages of each session is given and plotted with the fractionation factors of Pb and U in each session. The session number is given in the upper part of the diagram and lines have been drawn between the sessions to emphasise the changes between the sessions.*

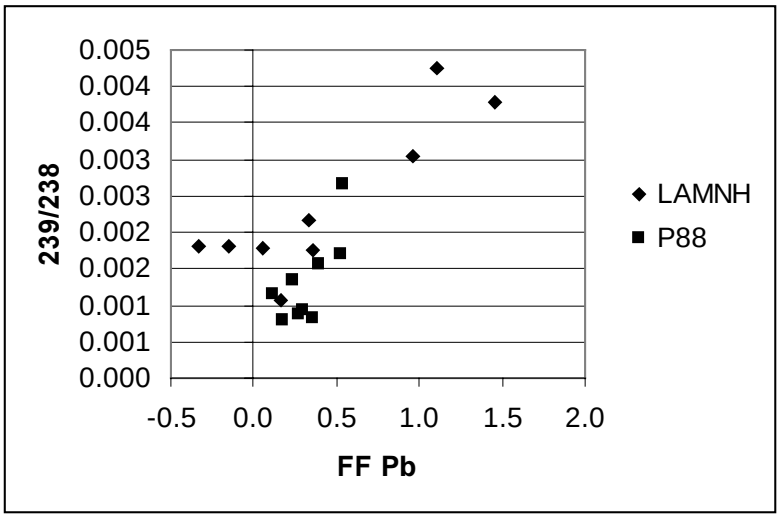

Figure 3-11. *Correlation between measured 239/238 and the apparent fractionation of Pb isotopes in uraninite (FF Pb). Positive FF indicates fractionation in favour of the heavier isotope, negative FF indicates fractionation in favour of the light isotope.*

4 Discussion

4.1 Lead

The results of this study regarding Pb isotopes in galena, show that there is significant fractionation of ca 0.5%/amu in favour of the light isotope. This is quite a high number, but it is reproduced in two laboratories and it is similar to the results of Meddaugh et al. /1982/, although Hart et al. /1981/ report fractionation of ca half of this magnitude.

Regarding uraninite, Holliger /1988/ found that Pb isotopes fractionate 0.35 ± 0.015%/amu (1σ) in favour of the lighter isotope, using a 50 eV energy offset. Cathelineau et al. /1990/, using an energy offset of 20 eV reported Pb isotope fractionations of 0.2%/amu in favour of the lighter isotope. In the present study, we have found that the Pb isotopic measurements have given relatively unstable results. Complicating factors may be non-homogeneity of the crystals themselves. However, for LAMNH-30222, two different areas of ca 0.2 mm in diameter each only differ 0.2% in the $^{207}Pb/^{206}Pb$, as measured by TIMS. This is less than the precision of the SIMS analysis.

There is a difference between the uraninite results at ORNL and the results at NORDSIM. On average, there is no fractionation of Pb isotopes at the ORNL laboratory, while at NORDSIM, the apparent fractionation varies between 0 and 2% in favour of the heavier isotope (average ca 1%). However, since most mass bias encountered during SIMS analyses favours the lighter isotope /Hinton, 1995/, the reverse mass bias calculated for Pb isotopic analysis at NORDSIM suggests that there was a problem with Pb-hydride interferences. Also, there are peaks at all masses where hydrides would be expected. The correlation between the measured amount of uranium hydrides, measured as $^{238}U^{1}H$, and the apparent Pb isotopic fractionation, is yet another argument for the interference of Pb-hydrides during the analysis. The lack of correlation between the Pb isotopic fractionation and the measured amounts of 209 is probably due to the existence of trace amounts of ^{209}Bi and/or REE-oxides.

The problem with hydride formation for precise Pb isotopic measurements has been known for some time /Long and Hinton, 1984; Williams, 1998/. Hydrides measured in ion microprobe analysis may have three origins: water present in the in the vacuum system, water on the sample surface, and water or hydroxide in the sample itself. Generally, the behaviour of Pb isotopes during different analytical conditions are similar for both standard uraninite crystals, as can be seen in Figure 3-8. One example is the excursion in session 13, which has a much higher fractionation that the other sessions. This implies that, at least during certain sessions, some of the factors involved are not related to the samples themselves, but to analytical conditions.

The analytical conditions and/or sample preparation at ORNL lessened the amount of measured hydrides. Vacuum pre-treatment of the sample minimises the water in the surface layer of the sample, and the cold trap minimises the hydrides found in the vacuum just around the sample. The 50 V offset should diminish the yield of molecular interferences; however, metal hydrides appear to have the same energy distribution as the metal ions /Long and Hinton, 1984; Hinton, 1995/, as can be seen in Figure 3-7. In spite of this, our results indicate that using energy filtering has an effect on the metal to metalhydride ratio.

Even if the reason for the effect of the 50 V offset is not evident, it seems obvious that it does diminish the UH/U. The correlation with low UH/U and low $^{207}Pb/^{206}Pb$ makes it reasonable to assume that the 50 V offset also diminishes the PbH. This is in agreement with the results of Long and Hinton /1984/, who observed that the ratio $(MH^+/M^+)_1/(MH^+/M^+)_2$ for two elements is shown to remain constant, irrespective of matrix and source of hydrogen. If this is the case, then one could estimate the hydride interference on Pb by measuring the amount of UH. This was in fact done by Reed et al. /1988/, who determined the (PbH/Pb)/(UH/U) to be 0.22 during pitchblende analyses. They found that the correction for pitchblende was on the order of 1%, which is of similar magnitude as the apparent fractionation in this study.

4.2 Uranium

A previous study of U isotope fractionation during ion microprobe analysis of uraninite /Holliger, 1992/ shows that the large fractionation of ca 2%/amu between U isotopes is reduced by measuring the uranium dioxide ion rather than metallic ion species. Our study shows that regardless of which U species is measured, a large fractionation exists for the U isotopes and that reproducibility is better for the metallic ion species. The fractionation we have calculated for the metallic U ion species is 1.4%/amu in favour of the lighter isotope, which is different than the previously reported value of 2.1%/amu /Holliger, 1992/. This large fractionation, however, can be slightly reduced using a 50 V energy offset. The fractionation of isotopes is usually expected to be low for very heavy elements due to the small relative difference in mass. Therefore, the large fractionation between U isotopes is surprising. Changes in instrumental conditions such as deadtime corrections and longer sputter-times, as well as monitoring crater depth and varying the primary beam current did not affect this large mass bias.

5 Conclusion

The fractionation of Pb isotopes measured in galena appears to be of similar magnitude in different laboratories, as well as constant between analytical sessions. The average from the three sessions, and three different isotope ratios at NORDSIM is a fractionation of 0.46±0.01%/amu (1σ) in favour of the lighter isotope. The average of ORNL sessions is 0.56±0.04%/amu (1σ). Hart et al. /1981/ reported a fractionation of smaller magnitude (0.25–0.35%/amu), while Meddaugh et al. /1982/ reported a fractionation of 0.48%/amu, in favour of the lighter isotope. This is similar to the ca 0.5%/amu found in the present study.

The fractionation of Pb isotopes in uraninite differs between laboratories. This is probably due to different amounts of measured hydrides, since the magnitude of the measured $^{207}Pb/^{206}Pb$ is positively correlated with the yield of mass 239 ($^{238}U^{1}H$). The hydride interferences can be minimised by using running at a 50 V offset, as well as using a cold trap and keeping the sample in vacuum for a number of days prior to analysis. Earlier studies appear not to have had the problem with hydride interferences, since they report a fractionation of 0.35% in favour of the lighter isotope /Cathelineau et al., 1990; Holliger, 1988/.

This study shows that there is a large fractionation of the U isotopes during SIMS-analyses, which appears to be similar in different laboratories. The agreement between the two laboratories, with a fractionation of 1.4±0.1%/amu (1σ) at Oak Ridge, and 1.4±0.4%/amu (1σ) at NORDSIM indicates that the fractionation of U isotopes during SIMS analyses of uraninite is approximately 1.4%/amu in favour of the lighter isotope. This number is large, but still less than the 2.1%/amu fractionation reported by Holliger /1992/.

The conclusions of this study are, therefore, that standard crystals of both galena and uraninite are needed to determine fractionation factors for Pb in galena and for U in uraninite during ion microprobe analysis. To measure the Pb isotopic composition of uraninite, the hydride interferences must be under control. The fractionation of Pb isotopes during ion microprobe analysis has not been determined in this study, due to problems probably related to hydride interferences. These problems may be minimised by subjecting the sample to vacuum for some days before analysis and using energy filtering and a cold trap during analysis.

6 Acknowledgements

We are grateful to Dan Holtstam, who provided the samples from the collections of Swedish Museum of Natural History, and informed us about the TIMS data of the galena. Thanks also go to Rod Ewing and Keld Alstrup Jensen, who found the promising sample UNM-337 in the collections of University of Michigan, and to LA Museum of Natural History for the access to the sample LAMNH-30222 which belongs to their collections. We also would like to thank the NORDSIM staff for assistance and helpful discussions. Lee R Riciputi helped us with the analyses at ORNL, for which we are grateful. The assistance of Hans Harryson at Uppsala University during electron microprobe analyses is greatly appreciated. Henrik Skogby och Roland Stalder are thanked for doing the IR analyses. This work was conducted while the first author was funded by the Swedish Nuclear Fuel and Waste Management (SKB).

References

Belshaw N S, O'Nions R K, Martel D J, Burton K W, 1994. High-resolution SIMS analysis of common lead. Chemical Geology, 112: 57–70.

Cathelineau M, Boiron M C, Holliger P, Poty B, 1990. Metallogenesis of the French part of the variscan orogen. Part II : Time-space relationships between U, Au and Sn-W ore deposition and geodynamic events -mineralogical and U-Pb data. Tectonophysics, 177: 59–79.

Davis G L, Tilton G R, Wetherill G W, 1962. Mineral ages from the Appalachian province in North Carolina and Tennessee. Journal of Geophysical Research, 67(5): 1987–1996.

Hart S R, Shimizu N, Sverjensky D A, 1981. Lead Isotope Zoning in Galena: An Ion Microprobe Study of a Galena Crystal from the Buick MIne, Southeast Missouri. Economic Geology, 76: 1873–1878.

Hervig R L, Williams P, Thomas R M, Schauer S N, Steele I M, 1992. Microanalysis of oxygen isotopes in insulators by secondary ion mass spectrometry. J. Mass. Spectrom. Ion Process., 120: 45–63.

Hinton R W, 1995. Ion microprobe analysis in geology. In: P J Potts, J F W Bowles, S J B Reed and M R Cave (Editors), Microprobe Techniques in the Earth Sciences. Chapman &Hall, pp. 235–289.

Holliger P, 1988. Ages U-Pb définis in-situ sur pechblende à l'analyseur ionique. C R Acad. Sci. Paris Ser.2, 307: 367–373.

Holliger P, 1992. SIMS isotope analysis of U and Pb in uranium oxides: geological and nuclear applications. In: A Benninghoven, K T F Jansen, J Tümpner and H W Werner (Editors), Secondary Ion Mass Spectrometry (SIMS VIII). John Wiley & Sons, Amsterdam, The Netherlands, pp. 719–722.

Holtstam D, Mansfeld J, 2001. Origin of a carbonate-hosted Fe-Mn-(Ba-As-Pb-Sb-W) deposit of Långban-type in central Sweden. Mineralium Deposita, 36: 641–657.

Long J V P, Hinton R H, 1984. The intensity of metal hydride peaks in secondary positive-ion spectra from silicates. International Journal of Mass Spectrometry and Ion Processes, 55: 307–318.

Ludwig K R, 1991. ISOPLOT; a plotting and regression program for radiogenic-isotope data; version 2.53. Open-File Report – U. S. Geological Survey. U. S. Geological Survey, Reston, VA, United States, 39 pp.

Lux D R, Guidotti C V, 1985. Evidence for extensive Hercynian metamorphism in western Maine. Geology (Boulder), 13(10): 696–700.

Lyon I C, Saxton J M, Turner G, 1994. Isotopic fractionation in secondary ionization mass spectrometry. Rapid Commun. Mass Spectrom., 8: 837–843.

Meddaugh W S, Holland H D, Shimizu N, 1982. The isotopic composition of lead in galenas in the uranium ores at Elliot Lake, Ontario, Canada. In: G C Amstutz et al. (Editors), Ore Genesis, the state of the art. Springer-Verlag, Berlin Heidelberg New York, pp. 25–37.

Reed S J B, Trueman N A, Long J V P, 1988. Ion microprobe U-Pb dating of pitchblende. In: A Benninghoven, A M Huber and H W Werner (Editors), Secondary Ion Mass Spectrometry (SIMS VI). John Wiley & Sons, Paris, France, pp. 945–948.

Shimizu N, Hart S R, 1982. Applications of the ion microprobe to geochemistry and cosmochemistry. Annual Review of Earth and Planetary Sciences, 10: 483–526.

Shroeer J M, Rhodin T N, Bradley R C, 1973. A quantum-mechanical model for the ionization and excitation of atoms during sputtering. Surface Science, 34: 571–580.

Sigmund P, 1969. Theory of sputtering, I. Sputtering yield of amorphous and polycrystalline targets. Phys. Rev., 184: 383–416.

Slodzian G, Lorin J C, Havette A, 1980. Isotopic effect on the ionization probabilities in secondary ion emission. Journal de Physique, Lettres, 41: L555–558.

Stacey J S, Kramers J D, 1975. Approximation of terrestial lead isotope evolution by a two-stage model. Earth and Planetary Science Letters, 26: 207–221.

Steiger R H, Jaeger E, 1977. Subcommission on geochronology; convention on the use of decay constants in geo- and cosmochronology. Earth and Planetary Science Letters, 36(3): 359–362.

Sundblad K, 1994. A genetic reinterpretation of the Falun and Åmmeberg ore types, Bergslagen, Sweden. Mineralium Deposita, 29: 170–179.

Valley J W, Graham C M, 1991. Ion microprobe analysis of oxygen isotope ratios in granulite facies magnetites; diffusive exchange as a guide to cooling history. Contributions to Mineralogy and Petrology, 109(1): 38–52.

Valley J W, Graham C M, Harte B, Eiler J M, Kinny P D, 1998. Ion microprobe analysis of oxygen, carbon, and hydrogen isotope ratios. In: M.A. McKibben, W.C. Shanks, III and W.I. Ridley (Editors), Applications of microanalytical techniques to understanding mineralizing processes. Reviews in Economic Geology. Society of Economic Geologists, Socorro, NM, United States, pp. 73–98.

Weathers D L, Spicklemire S J, Tombrello T A, Hutcheon I D, Gnaser H, 1993. Isotopic fractionation in the sputtering of 92Mo-100Mo targets. Nuclear Instruments and Methods, B73: 135–150.

Welin E, Blomqvist G, 1964. Age measurements on radioactive minerals from Sweden. GFF, 86: 33–50.

Williams P, 1979. The sputtering process and sputtered ion emission. Surface Science, 90: 588–643.

Williams, I S, 1998. U-Th-Pb geochronology by ion microprobe. Reviews in Economic Geology, 7: 1–35.

Yu M L, Lang N, 1986. Mechanisms of atomic ion emission during sputtering. Nuclear Instruments and Methods, B14: 403–413.

Appendix

Table A-1. SIMS Pb isotopic data of NRM-990118 galena. Errors are 1σ, and the error on the average is the standard deviation of the session.

File	206/204	±	207/206	±	208/206	±
TIMS	15.736	0.011	0.976	0.002	2.241	0.005
Session OR-1						
1-3PB11	15.521	0.0184	0.972	0.0007		
1-3PB12	15.554	0.0194	0.970	0.0008	2.213	0.0035
1-3PB13	15.521	0.0143	0.971	0.0006	2.211	0.0013
1-3PB14	15.507	0.0080	0.972	0.0004	2.216	0.0015
1-3PB15	15.492	0.0160	0.971	0.0007	2.211	0.0008
Average 1	15.519	0.0231	0.971	0.0008	2.213	0.0023
Session OR-2						
1-4PB1	15.506	0.0238	0.972	0.0011	2.220	0.0022
1-4PB2	15.549	0.1347	0.972	0.0006	2.218	0.0041
1-4PB3	15.530	0.0746	0.972	0.0009	2.221	0.0033
1-4PB4	15.531	0.0692	0.971	0.0006	2.212	0.0028
1-4PB5	15.513	0.0807	0.972	0.0006	2.224	0.0025
Average 2	15.526	0.0168	0.972	0.0006	2.219	0.0042
Session OR-3						
1-5PB11	15.525	0.1433	0.972	0.0009	2.213	0.0076
1-5PB12	15.494	0.0270	0.972	0.0004	2.214	0.0010
1-5PB13	15.580	0.0865	0.972	0.0010	2.213	0.0051
1-5PB14	15.517	0.0807	0.973	0.0014	2.215	0.0048
1-5PB15	15.577	0.1127	0.973	0.0014	2.217	0.0055
Average 3	15.539	0.0381	0.972	0.0006	2.214	0.0015
Session 11						
n821-03a	15.510	0.088	0.977	0.004	2.224	0.007
n821-03b	15.620	0.056	0.971	0.003	2.224	0.006
n821-03c	15.620	0.042	0.970	0.002	2.217	0.005
n821-03d	15.640	0.030	0.972	0.002	2.220	0.004
n821-03e	15.550	0.039	0.973	0.002	2.223	0.003
n821-03f	15.650	0.029	0.966	0.002	2.220	0.004
n821-03g	15.660	0.035	0.973	0.002	2.219	0.004
n821-03h	15.580	0.039	0.974	0.002	2.219	0.003
n821-03i	15.570	0.032	0.971	0.002	2.224	0.004
n821-03j	15.600	0.040	0.968	0.002	2.221	0.005
Average 11	15.600	0.048	0.971	0.003	2.221	0.003
Session 12						
n821-03k	15.600	0.034	0.969	0.002	2.220	0.004
n821-03l	15.570	0.050	0.971	0.002	2.223	0.004
n821-03m	15.560	0.035	0.972	0.002	2.223	0.004
n821-03n	15.600	0.038	0.973	0.002	2.219	0.003
n821-03o	15.600	0.032	0.973	0.002	2.221	0.005
n821-03p	15.620	0.033	0.969	0.002	2.220	0.004
n821-03q	15.610	0.038	0.972	0.002	2.219	0.004
n821-03r	15.530	0.043	0.975	0.003	2.226	0.005
Average 12	15.586	0.030	0.972	0.002	2.221	0.002

Table A-1 (contd.)

File	206/204	±	207/206	±	208/206	±
Session 13						
n821-03s	15.600	0.042	0.967	0.002	2.221	0.004
n821-03t	15.560	0.041	0.977	0.002	2.225	0.004
n821-03u	15.590	0.035	0.970	0.002	2.221	0.004
n821-03v	15.590	0.041	0.974	0.002	2.219	0.005
n821-03x	15.540	0.042	0.971	0.002	2.221	0.004
n821-03y	15.520	0.037	0.976	0.002	2.218	0.004
n821-03z	15.570	0.029	0.968	0.002		
Average 13	15.567	0.029	0.972	0.004	2.219	0.005

Table A-2. SIMS isotopic data of uraninite P88. Errors are 1σ, and the error on the average of each session is the standard deviation of the session. Italic font indicates that the uranium oxide ion has been measured. If 204/206 is less than 0.0000005, the value has been approximated to 0. f= fraction of common Pb, 207/206* = corrected for common Pb.

File	204/206	±	207/206	±	f	±	207/206*	±	208/206	±	235/238	±
TIMS	0.00002	0.00000				0.0692	0.00003	0.02049	0.00003	0.0073	0	
Session OR-1												
1-3PB6	0.00002	0.00000	0.0693	0.00006	0.00039	0.00001	0.0690	0.00006	0.0210	0.00002		
1-3PB7	0.00002	0.00000	0.0692	0.00006	0.00038	0.00001	0.0689	0.00006	0.0212	0.00001	0.00763	0.00003
1-3PB8	0.00002	0.00000	0.0694	0.00004	0.00038	0.00001	0.0691	0.00004	0.0202	0.00001	0.00756	0.00002
1-3PB9	0.00002	0.00000	0.0693	0.00005	0.00037	0.00001	0.0690	0.00005	0.0199	0.00001	0.00756	0.00002
1-3PB10	0.00002	0.00000	0.0693	0.00006	0.00038	0.00001	0.0690	0.00006	0.0198	0.00001	0.00764	0.00002
Average 1	0.00002	0.00000	0.0693	0.00008			0.0690	0.00008	0.0204	0.00067	0.00760	0.00004
Session OR-2												
1-4PB12	0.00003	0.00000	0.0693	0.00006	0.00052	0.00002	0.0689	0.00006	0.0213	0.00002	0.00762	0.00003
1-4PB13	0.00003	0.00000	0.0694	0.00008	0.00048	0.00001	0.0691	0.00008	0.0204	0.00002	0.00756	0.00002
1-4PB14	0.00003	0.00000	0.0693	0.00010	0.00052	0.00002	0.0689	0.00010	0.0204	0.00002	0.00761	0.00003
1-4PB15	0.00003	0.00000	0.0694	0.00009	0.00052	0.00001	0.0690	0.00009	0.0205	0.00003	0.00759	0.00003
1-4PB16	0.00003	0.00000	0.0694	0.00013	0.00054	0.00002	0.0690	0.00013	0.0212	0.00005	0.00755	0.00002
Average 2	0.00003	0.00000	0.0694	0.00006			0.0690	0.00006	0.0208	0.00046	0.00759	0.00003
Session OR-3												
1-5PB1	0.00003	0.00000	0.0694	0.00007	0.00051	0.00002	0.0690	0.00007	0.0201	0.00002	0.00766	0.00004
1-5PB2	0.00003	0.00000	0.0693	0.00012	0.00050	0.00001	0.0690	0.00012	0.0213	0.00001	0.00757	0.00002
1-5PB3	0.00003	0.00000	0.0694	0.00009	0.00055	0.00001	0.0689	0.00009	0.0214	0.00002	0.00762	0.00003
1-5PB4	0.00003	0.00000	0.0695	0.00012	0.00047	0.00002	0.0692	0.00012	0.0218	0.00002	0.00754	0.00002
1-5PB5	0.00003	0.00000	0.0695	0.00008	0.00050	0.00001	0.0692	0.00008	0.0217	0.00003	0.00764	0.00003
Average 3	0.00003	0.00000	0.0694	0.00009			0.0690	0.00011	0.0213	0.00066	0.00761	0.00005
Session 1												
n376-01a			0.0703	0.00018					0.0200	0.00010	0.00766	0.00005
n376-01b			0.0699	0.00008					0.0205	0.00003	0.00767	0.00005
n376-01c			0.0702	0.00007					0.0215	0.00003	0.00773	0.00004
n376-01d									0.0207	0.00006	0.00759	0.00004
n376-01e			0.0695	0.00028					0.0208	0.00008	0.00763	0.00004
n376-01f			0.0700	0.00008					0.0213	0.00004	0.00770	0.00004
n376-01g			0.0701	0.00025					0.0213	0.00017	0.00752	0.00007
n376-01i			0.0696	0.00012					0.0211	0.00005	0.00760	0.00007
n376-01k			0.0697	0.00010					0.0204	0.00005	0.00755	0.00008
n376-01l			0.0697	0.00009					0.0209	0.00006	0.00762	0.00009
n376-01m			0.0697	0.00009					0.0211	0.00004	0.00765	0.00008
n376-01n			0.0698	0.00011					0.0215	0.00003	0.00769	0.00009
n376-01o			0.0698	0.00004					0.0215	0.00003	0.00757	0.00010
n376-01p			0.0697	0.00015					0.0214	0.00004	0.00765	0.00005
n376-01q			0.0696	0.00008					0.0212	0.00003	0.00773	0.00009
n376-01r			0.0697	0.00011					0.0210	0.00012	0.00761	0.00005
n376-01s			0.0699	0.00010					0.0205	0.00003	0.00781	0.00008
Average 1			0.0698	0.00023					0.0210	0.00045	0.00765	0.00007
Session 2												
n376-02a			0.0693	0.00008					0.0195	0.00003	0.00747	0.00004
n376-02b			0.0696	0.00011					0.0196	0.00007	0.00775	0.00012
n376-02c			0.0692	0.00014					0.0198	0.00004	0.00783	0.00012
n376-02d			0.0694	0.00005					0.0196	0.00004	0.00776	0.00011
n376-02e			0.0696	0.00006					0.0196	0.00007	0.00765	0.00007
n376-02f			0.0695	0.00014					0.0196	0.00003	0.00756	0.00008
n376-02g			0.0696	0.00010					0.0199	0.00007	0.00770	0.00005
n376-02h			0.0697	0.00008					0.0197	0.00003	0.00759	0.00005
n376-02i			0.0697	0.00006					0.0200	0.00003	0.00760	0.00003
n376-02k			0.0698	0.00010					0.0200	0.00004	0.00754	0.00003
n376-02l			0.0699	0.00012					0.0204	0.00005	0.00769	0.00006

Table A-2 (contd.)

File	204/206	±	207/206	±	f	±	207/206*	±	208/206	±	235/238	±
Session 2 (forts)												
n376-02m			0.0697	0.00010					0.0203	0.00004	0.00757	0.00005
n376-02n			0.0698	0.00012					0.0212	0.00005	0.00757	0.00003
n376-02o			0.0698	0.00007					0.0212	0.00003	0.00757	0.00005
n376-02p			0.0697	0.00009					0.0211	0.00004	0.00750	0.00004
n376-02q			0.0699	0.00010					0.0209	0.00006	0.00763	0.00005
n376-02r			0.0697	0.00011					0.0211	0.00006	0.00765	0.00003
n376-02s			0.0700	0.00011					0.0211	0.00004	0.00762	0.00004
n376-02t			0.0696	0.00021					0.0208	0.00008	0.00785	0.00012
n376-02u			0.0694	0.00006					0.0206	0.00005	0.00769	0.00008
n376-02v			0.0699	0.00011					0.0208	0.00009	0.00743	0.00005
n376-02x			0.0696	0.00013					0.0207	0.00006	0.00762	0.00005
n376-02y			0.0697	0.00013					0.0207	0.00004	0.00786	0.00006
n376-02z			0.0697	0.00019					0.0209	0.00005	0.00779	0.00012
Average 2			0.0697	0.00019					0.0204	0.00061	0.00765	0.00012
Session 3												
n376-03a	0.00267	0.00001	0.0707	0.00014	0.04604	0.00023	0.0326	0.00015	0.0188	0.00005	*0.00753*	*0.00002*
n376-03b	0.00269	0.00001	0.0717	0.00013	0.04636	0.00020	0.0334	0.00014	0.0200	0.00005	*0.00753*	*0.00002*
n376-03c	0.00225	0.00003			0.03877	0.00056	-0.0346	0.00002	0.0201	0.00010	*0.00762*	*0.00002*
n376-03d	0.00366	0.00007			0.06304	0.00125	-0.0578	0.00007	0.0142	0.00021	*0.00756*	*0.00002*
n376-03e	0.00276	0.00001	0.0719	0.00018	0.04754	0.00019	0.0326	0.00019	0.0215	0.00005	*0.00759*	*0.00002*
n376-03f	0.00241	0.00001	0.0710	0.00017	0.04144	0.00016	0.0370	0.00018	0.0209	0.00010	*0.00709*	*0.00003*
n376-03g	0.00305	0.00002	0.0725	0.00014	0.05244	0.00040	0.0289	0.00015	0.0206	0.00009	*0.00746*	*0.00002*
n376-03h	0.00215	0.00001	0.0701	0.00013	0.03698	0.00018	0.0398	0.00014	0.0207	0.00010	*0.00738*	*0.00002*
n376-03i	0.00222	0.00001	0.0713	0.00009	0.03815	0.00012	0.0400	0.00010	0.0207	0.00004	*0.00753*	*0.00002*
n376-03k	0.00223	0.00001	0.0707	0.00007	0.03839	0.00011	0.0392	0.00007	0.0205	0.00003	*0.00752*	*0.00001*
Average 3	0.00261	0.00047	0.0712	0.00076			0.0191	0.03506	0.0198	0.00207	*0.00748*	*0.00015*
Session 4												
n376-04a	0.00215	0.00001	0.0709	0.00007	0.03705	0.00016	0.0406	0.00007	0.0206	0.00003		
n376-04b	0.00222	0.00001	0.0712	0.00009	0.03817	0.00018	0.0400	0.00009	0.0207	0.00003	*0.00763*	*0.00011*
Average 4	0.00218	0.00005	0.0711	0.00025			0.0403	0.00042	0.0206	0.00010		
Session 5												
n376-05a	0.00102	0.00005	0.0672	0.00051	0.01753	0.00078	0.0531	0.00052	0.0191	0.00026	*0.00714*	*0.00007*
n376-05b	0.00076	0.00005	0.0808	0.00098	0.01316	0.00088	0.0704	0.00100	0.0234	0.00043	*0.00855*	*0.00011*
n376-05c	0.00095	0.00004	0.0714	0.00048	0.01630	0.00075	0.0583	0.00049	0.0219	0.00028	*0.00752*	*0.00006*
n376-05d	0.00111	0.00010	0.0762	0.00082	0.01903	0.00165	0.0610	0.00085	0.0214	0.00046	*0.00808*	*0.00018*
Average 5	0.00096	0.00014	0.0739	0.00587			0.0607	0.00725	0.0215	0.00181	*0.00782*	*0.00062*
Session 6												
n376-06a	0.00256	0.00016	0.0745	0.00131	0.04406	0.00267	0.0384	0.00137	0.0204	0.00035	*0.00674*	*0.00013*
n376-06b	0.00067	0.00007	0.0732	0.00105	0.01146	0.00127	0.0641	0.00106	0.0230	0.00048	*0.00752*	*0.00009*
n376-06c	0.00309	0.00011	0.0748	0.00054	0.05320	0.00198	0.0308	0.00057	0.0230	0.00028	*0.00740*	*0.00012*
n376-06d	0.00302	0.00005	0.0700	0.00055	0.05196	0.00082	0.0267	0.00058	0.0229	0.00023	*0.00769*	*0.00009*
Average 6	0.00233	0.00114	0.0731	0.00222			0.0400	0.01676	0.0223	0.00128	*0.00734*	*0.00041*
Session 12												
n821-04a	0.00000		0.0698	0.00012	0.00000	0.00000	0.0698	0.00012	0.0203	0.00004	0.00756	0.00011
n821-04b	0.00000		0.0694	0.00015	0.00000	0.00000	0.0694	0.00015	0.0202	0.00007	0.00766	0.00013
n821-04c	0.00000		0.0696	0.00012	0.00001	0.00000	0.0696	0.00012	0.0207	0.00006	0.00767	0.00009
n821-04d	0.00000		0.0700	0.00013	0.00001	0.00000	0.0700	0.00013	0.0200	0.00008	0.00747	0.00016
n821-04e	0.00000		0.0700	0.00011	0.00000	0.00000	0.0700	0.00011	0.0206	0.00005	0.00772	0.00011
Average 12			0.0698	0.00027			0.0697	0.00027	0.0204	0.00026	0.00762	0.00010
Session 13												
n821-04f	0.00000		0.0708	0.00008	0.00000	0.00000	0.0708	0.00008	0.0200	0.00002	0.00759	0.00003
n821-04g	0.00000		0.0706	0.00007	0.00000	0.00000	0.0706	0.00007	0.0206	0.00003	0.00760	0.00003
n821-04h	0.00000		0.0709	0.00009	0.00001	0.00000	0.0709	0.00009	0.0213	0.00003	0.00762	0.00002
n821-04i	0.00000		0.0703	0.00008	0.00000	0.00000	0.0703	0.00008	0.0207	0.00003	0.00769	0.00003
Average 13			0.0706	0.00023			0.0706	0.00023	0.0206	0.00055	0.00762	0.00004

Table A-2 (contd.)

File	204/206	±	207/206	±	f	±	207/206*	±	208/206	±	235/238	±
Session 14												
n821-06a	0.00000		0.0657	0.00020	0.00000	0.00000	0.0657	0.00020	0.0204	0.00005	0.00753	0.00003
n821-06b	0.00000		0.0648	0.00019	0.00001	0.00000	0.0648	0.00019	0.0234	0.00013	0.00740	0.00004
n821-06c	0.00000		0.0649	0.00019	0.00001	0.00000	0.0648	0.00019	0.0210	0.00007	0.00748	0.00004
n821-06d	0.00000		0.0682	0.00018	0.00000	0.00000	0.0682	0.00018	0.0206	0.00005	0.00751	0.00003
n821-06e	0.00000		0.0669	0.00021	0.00001	0.00000	0.0669	0.00021	0.0193	0.00006	0.00762	0.00004
n821-06f	0.00000		0.0677	0.00023	0.00001	0.00000	0.0677	0.00023	0.0213	0.00006	0.00756	0.00004
n821-06g	0.00000		0.0684	0.00013	0.00000	0.00000	0.0684	0.00013	0.0201	0.00006	0.00760	0.00004
n821-06h	0.00000		0.0691	0.00023	0.00000	0.00000	0.0691	0.00023	0.0204	0.00007	0.00755	0.00004
Average 14			0.0670	0.00166			0.0670	0.00166	0.0208	0.00121	0.00753	0.00007
Session 16												
n911-02a	0.00000	0.00000			0.00000	0.00000	0.0000	0.00000	0.0206	0.00009	0.00749	0.00006
n911-02e	0.00022	0.00000	0.0696	0.00012	0.00384	0.00003	0.0666	0.00012	0.0212	0.00003	0.00760	0.00003
n911-02f	0.00023	0.00000	0.0695	0.00006	0.00389	0.00003	0.0664	0.00006	0.0211	0.00003	0.00759	0.00003
n911-02g	0.00022	0.00000	0.0696	0.00008	0.00376	0.00003	0.0666	0.00008	0.0208	0.00001	0.00755	0.00005
Average 16	0.00022	0.00000	0.0696	0.00010			0.0499	0.03326	0.0210	0.00021	0.00758	0.00003
Session 17												
n911-02h	0.00000	0.00000	0.0695	0.00007	0.00001	0.00000	0.0695	0.00007	0.0211	0.00002	0.00752	0.00002
n911-02l	0.00000	0.00000	0.0696	0.00008	0.00001	0.00000	0.0696	0.00008	0.0210	0.00003	0.00753	0.00005
n911-02m	0.00000	0.00000	0.0694	0.00006	0.00001	0.00000	0.0694	0.00006	0.0215	0.00002	0.00748	0.00003
n911-02n	0.00000	0.00000	0.0694	0.00007	0.00001	0.00000	0.0694	0.00007	0.0201	0.00002	0.00758	0.00003
n911-02o	0.00000	0.00000	0.0695	0.00008	0.00000	0.00000	0.0695	0.00008	0.0201	0.00002	0.00754	0.00006
n911-02p	0.00000	0.00000	0.0694	0.00009	0.00001	0.00000	0.0694	0.00009	0.0200	0.00002	0.00760	0.00003
Average 17	0.00000	0.00000	0.0695	0.00008			0.0695	0.00008	0.0206	0.00065	0.00754	0.00004
Session 18a												
n911-04a	0.00000	0.00000	0.0694	0.00024	0.00000	0.00000	0.0693	0.00024	0.0210	0.00007	0.00748	0.00001
n911-04b	0.00000	0.00000	0.0695	0.00029	0.00001	0.00001	0.0695	0.00029	0.0214	0.00008	0.00752	0.00002
n911-04c	0.00000	0.00000	0.0693	0.00016	0.00000	0.00000	0.0693	0.00016	0.0212	0.00009	0.00755	0.00002
n011-04d	0.00000	0.00000	0.0687	0.00028	0.00000	0.00000	0.0687	0.00028	0.0211	0.00006	0.00752	0.00001
n911-04f	0.00000	0.00000	0.0692	0.00021	0.00001	0.00000	0.0692	0.00021	0.0200	0.00008	0.00752	0.00002
n911-04g	0.00000	0.00000	0.0699	0.00028	0.00001	0.00001	0.0699	0.00028	0.0195	0.00011	0.00752	0.00002
n911-04h	0.00000	0.00000	0.0690	0.00028	0.00000	0.00000	0.0690	0.00028	0.0211	0.00010	0.00751	0.00001
Average 18a	0.00000	0.00000	0.0693	0.00039			0.0693	0.00038	0.0208	0.00070	0.00752	0.00002
Session 18b												
n911-04i	0.00000	0.00000	0.0695	0.00009	0.00001	0.00000	0.0695	0.00009	0.0208	0.00002	0.00760	0.00004
n911-04j	0.00000	0.00000	0.0696	0.00010	0.00001	0.00000	0.0696	0.00010	0.0202	0.00003	0.00751	0.00005
n911-04k	0.00000	0.00000	0.0696	0.00007	0.00001	0.00000	0.0696	0.00007	0.0213	0.00002	0.00759	0.00004
Average 18b	0.00000	0.00000	0.0696	0.00008			0.0696	0.00008	0.0208	0.00057	0.00757	0.00005
Session 19												
n911-07a	0.00000	0.00000	0.0694	0.00005	0.00001	0.00000	0.0694	0.00005	0.0212	0.00002	0.00758	0.00002
n911-07f	0.00000	0.00000	0.0695	0.00010	0.00000	0.00000	0.0695	0.00010	0.0211	0.00003	0.00753	0.00002
n911-07g	0.00000	0.00000	0.0692	0.00010	0.00001	0.00000	0.0692	0.00010	0.0209	0.00004	0.00756	0.00002
n911-07h	0.00000	0.00000	0.0693	0.00009	0.00002	0.00000	0.0693	0.00009	0.0211	0.00003	0.00756	0.00004
n911-07i	0.00000	0.00000	0.0694	0.00010	0.00001	0.00000	0.0694	0.00010	0.0212	0.00004	0.00756	0.00003
n911-07j	0.00000	0.00000	0.0693	0.00007	0.00000	0.00000	0.0693	0.00007	0.0213	0.00003	0.00759	0.00002
Average 19	0.00000	0.00000	0.0694	0.00011			0.0694	0.00011	0.0211	0.00014	0.00756	0.00002
Session 20												
n911-07k	0.00000	0.00000	0.0696	0.00021	0.00000	0.00000	0.0695	0.00021	0.0210	0.00013	0.00751	0.00002
n911-07l	0.00000	0.00000	0.0695	0.00017	0.00000	0.00000	0.0695	0.00017	0.0210	0.00008	0.00750	0.00001
n911-07m	0.00000	0.00000	0.0695	0.00030	0.00000	0.00001	0.0695	0.00030	0.0213	0.00010	0.00752	0.00001
n911-07n	0.00000	0.00000	0.0690	0.00018	0.00000	0.00000	0.0690	0.00018	0.0205	0.00009	0.00754	0.00002
Average 20	0.00000	0.00000	0.0694	0.00025			0.0694	0.00025	0.0209	0.00033	0.00752	0.00002

Table A-3. SIMS isotopic data of uraninite LAMNH-30222. Errors are 1σ, and the error on the average of each session is the standard deviation of the session. Italic font indicates that the uranium dioxide ion has been measured. If 204/206 is less than 0.0000005, the value has been approximated to 0. f= fraction of common Pb, 207/206* =corrected for common Pb.

File	204/206	±	207/206	±	f	±	207/206*	±	208/206	±	235/238	±
TIMS			0.0538	0.00006			0.0538	0.00006	0.00261	0.00006	0.00725	0
Session OR-1												
1-3PB1	0.00000	0.000000	0.05391	0.00006	0.00008	0.00001	0.05385	0.00006	0.00279	0.00001	0.00751	0.00001
1-3PB2	0.00001	0.000000	0.05387	0.00006	0.00012	0.00001	0.05378	0.00006	0.00275	0.00001	0.00757	0.00002
1-3PB3	0.00001	0.000001	0.05373	0.00006	0.00012	0.00001	0.05364	0.00006	0.00252	0.00001	0.00759	0.00002
1-3PB4	0.00001	0.000001	0.05370	0.00007	0.00011	0.00001	0.05361	0.00007	0.00242	0.00002	0.00753	0.00002
1-3PB5	0.00000	0.000000	0.05381	0.00006	0.00006	0.00000	0.05376	0.00006	0.00228	0.00001	0.00754	0.00002
Session OR-2												
Average 1	0.00001	0.000001	0.05380	0.00009			0.05372	0.00010	0.00255	0.00022	0.00755	0.00003
1-4PB6	0.00003	0.000001	0.05431	0.00007	0.00055	0.00002	0.05387	0.00007	0.00274	0.00003	0.00769	0.00003
1-4PB7	0.00003	0.000001	0.05431	0.00006	0.00053	0.00002	0.05388	0.00006	0.00325	0.00002	0.00757	0.00002
1-4PB8	0.00004	0.000003	0.05454	0.00012	0.00075	0.00006	0.05394	0.00012	0.00357	0.00013	0.00757	0.00002
1-4PB9	0.00003	0.000001	0.05434	0.00011	0.00056	0.00002	0.05388	0.00011	0.00319	0.00001	0.00751	0.00003
1-4PB10	0.00002	0.000001	0.05408	0.00008	0.00038	0.00001	0.05378	0.00008	0.00276	0.00002	0.00764	0.00005
1-4PB11	0.00003	0.000001	0.05415	0.00009	0.00061	0.00001	0.05366	0.00009	0.00332	0.00003	0.00760	0.00003
Average 2	0.00003	0.000007	0.05429	0.00016			0.05384	0.00010	0.00314	0.00033	0.00760	0.00006
Session OR-3												
1-5PB6	0.00002	0.000001	0.05390	0.00011	0.00028	0.00002	0.05367	0.00011	0.00269	0.00001	0.00748	0.00004
1-5PB7	0.00001	0.000001	0.05378	0.00005	0.00025	0.00002	0.05358	0.00005	0.00263	0.00003	0.00751	0.00002
1-5PB8	0.00001	0.000001	0.05391	0.00012	0.00023	0.00002	0.05372	0.00012	0.00261	0.00001	0.00755	0.00002
1-5PB9	0.00001	0.000000	0.05375	0.00011	0.00022	0.00001	0.05357	0.00011	0.00245	0.00001	0.00756	0.00004
1-5PB10	0.00001	0.000001	0.05380	0.00016	0.00024	0.00002	0.05361	0.00016	0.00270	0.00002	0.00755	0.00003
Average 3	0.00001	0.000001	0.05383	0.00007			0.05363	0.00006	0.00261	0.00010	0.00753	0.00003
Session 7												
LA30222-0001	0.00000		0.05344	0.00024	0.00006	0.00000	0.05339	0.00024	0.00204	0.00004	*0.00761*	*0.00003*
LA30222-0002	0.00000		0.05375	0.00021	0.00000	0.00000	0.05375	0.00021	0.00244	0.00004	*0.00718*	*0.00003*
LA30222-0003	0.00000		0.05518	0.00027	0.00000	0.00000	0.05518	0.00027	0.00229	0.00002	*0.00768*	*0.00004*
LA30222-0004	0.00000		0.05503	0.00034	0.00000	0.00000	0.05503	0.00034	0.00197	0.00003	*0.00738*	*0.00007*
Average 7	0.00000	0.000002	0.05435	0.00088			0.05434	0.00090	0.00218	0.00022	*0.00746*	*0.00023*
Session 8												
LA30222-0005	0.00000	0.000000	0.05434	0.00023	0.00000	0.00000	0.05434	0.00023	0.00228	0.00002	*0.00725*	*0.00002*
LA30222-0006	0.00000	0.000002	0.05461	0.00009	0.00000	0.00003	0.05461	0.00009	0.00227	0.00002	*0.00748*	*0.00002*
LA30222-0007	0.00000	0.000000	0.05217	0.00023	0.00000	0.00000	0.05217	0.00023	0.00224	0.00004	*0.00739*	*0.00003*
LA30222-0008	0.00000	0.000000	0.05206	0.00015	0.00000	0.00000	0.05206	0.00015	0.00226	0.00003	*0.00741*	*0.00003*
LA30222-0009	0.00000	0.000001	0.05390	0.00013	0.00000	0.00001	0.05390	0.00013	0.00235	0.00003	*0.00742*	*0.00003*
LA30222-0010	0.00000	0.000000	0.05378	0.00013	0.00000	0.00000	0.05378	0.00013	0.00221	0.00001	*0.00751*	*0.00003*
LA30222-0011	0.00000	0.000000	0.05384	0.00030	0.00000	0.00000	0.05384	0.00030	0.00263	0.00003	*0.00747*	*0.00003*
LA30222-0012	0.00000	0.000000	0.05363	0.00023	0.00000	0.00000	0.05363	0.00023	0.00250	0.00002	*0.00745*	*0.00004*
LA30222-0013	0.00000	0.000001	0.05224	0.00042	0.00003	0.00002	0.05222	0.00042	0.00223	0.00004	*0.00769*	*0.00005*
LA30222-0014	0.00000	0.000000	0.05305	0.00020	0.00000	0.00000	0.05305	0.00020	0.00208	0.00003	*0.00762*	*0.00005*
LA30222-0015	0.00000	0.000001	0.05398	0.00024	0.00007	0.00002	0.05393	0.00024	0.00270	0.00003	*0.00735*	*0.00003*
LA30222-0016	0.00000	0.000001	0.05217	0.00046	0.00004	0.00002	0.05214	0.00046	0.00263	0.00007	*0.00750*	*0.00004*
LA30222-0017	0.00000	0.000000	0.05301	0.00047	0.00000	0.00001	0.05301	0.00047	0.00273	0.00004	*0.00753*	*0.00003*
LA30222-0018	0.00000	0.000001	0.05410	0.00024	0.00001	0.00001	0.05409	0.00024	0.00240	0.00002	*0.00742*	*0.00004*
LA30222-0019	0.00000	0.000001	0.05394	0.00027	0.00003	0.00001	0.05391	0.00027	0.00255	0.00002	*0.00742*	*0.00005*
LA30222-0020	0.00000	0.000000	0.05240	0.00034	0.00000	0.00000	0.05240	0.00034	0.00191	0.00003	*0.00730*	*0.00004*
LA30222-0021	0.00000	0.000000	0.05424	0.00038	0.00000	0.00000	0.05424	0.00038	0.00183	0.00003	*0.00733*	*0.00004*
LA30222-0022	0.00000	0.000000	0.05390	0.00036	0.00000	0.00000	0.05390	0.00036	0.00168	0.00003	*0.00754*	*0.00006*
LA30222-0023	0.00000	0.000000	0.05383	0.00031	0.00000	0.00001	0.05383	0.00031	0.00215	0.00003	*0.00761*	*0.00004*
LA30222-0024	0.00000	0.000000	0.05402	0.00047	0.00000	0.00000	0.05402	0.00047	0.00207	0.00003	*0.00768*	*0.00004*

Table A-3 (contd.)

File	204/206	±	207/206	±	f	±	207/206*	±	208/206	±	235/238	±
Session 8 (contd.)												
LA30222-0025	0.00000	0.000000	0.05413	0.00071	0.00000	0.00000	0.05413	0.00071	0.00205	0.00003	*0.00743*	*0.00004*
LA30222-0026	0.00000	0.000000	0.05450	0.00042	0.00000	0.00000	0.05450	0.00042	0.00212	0.00002	*0.00736*	*0.00007*
Average 8	0.00000	0.000001	0.05354	0.00083			0.05353	0.00083	0.00227	0.00028	*0.00746*	*0.00012*
Session 9												
LA30222-0027	0.00000	0.000000	0.05412	0.00024	0.00000	0.00000	0.05412	0.00024	0.00218	0.00003	*0.00741*	*0.00005*
LA30222-0028	0.00000	0.000000	0.05423	0.00043	0.00000	0.00000	0.05423	0.00043	0.00211	0.00002	*0.00768*	*0.00003*
LA30222-0029	0.00000	0.000000	0.05439	0.00043	0.00000	0.00000	0.05439	0.00043	0.00213	0.00003	*0.00760*	*0.00003*
LA30222-0030	0.00000	0.000000	0.05341	0.00045	0.00000	0.00001	0.05341	0.00045	0.00185	0.00004	*0.00746*	*0.00007*
LA30222-0031	0.00000	0.000000	0.05349	0.00056	0.00000	0.00000	0.05349	0.00056	0.00174	0.00003	*0.00748*	*0.00004*
LA30222-0032	0.00000	0.000000	0.05368	0.00042	0.00000	0.00000	0.05368	0.00042	0.00181	0.00001	*0.00744*	*0.00002*
LA30222-0033	0.00000	0.000001	0.05402	0.00032	0.00000	0.00003	0.05402	0.00032	0.00184	0.00002	*0.00720*	*0.00004*
LA30222-0034	0.00000	0.000000	0.05501	0.00017	0.00000	0.00000	0.05501	0.00017	0.00181	0.00002	*0.00726*	*0.00003*
LA30222-0035	0.00000	0.000000	0.05431	0.00019	0.00000	0.00000	0.05431	0.00019	0.00185	0.00002	*0.00724*	*0.00003*
LA30222-0036	0.00000	0.000000	0.05246	0.00036	0.00000	0.00000	0.05246	0.00036	0.00226	0.00004	*0.00762*	*0.00003*
LA30222-0037	0.00000	0.000000	0.05384	0.00012	0.00000	0.00000	0.05384	0.00012	0.00215	0.00001	*0.00741*	*0.00001*
LA30222-0038	0.00000	0.000000	0.04886	0.00027	0.00000	0.00000			0.00192	0.00002	*0.00716*	*0.00004*
LA30222-0039	0.00000	0.000000	0.05361	0.00036	0.00000	0.00000	0.05361	0.00036	0.00194	0.00003	*0.00757*	*0.00003*
LA30222-0040	0.00000	0.000000	0.05252	0.00035	0.00000	0.00000	0.05252	0.00035	0.00184	0.00003	*0.00724*	*0.00002*
LA30222-0041	0.00000	0.000000	0.04980	0.00031	0.00000	0.00001			0.00166	0.00004	*0.00743*	*0.00003*
LA30222-0042	0.00000	0.000000	0.05358	0.00061	0.00000	0.00001	0.05358	0.00061	0.00134	0.00003	*0.00737*	*0.00003*
LA30222-0043	0.00000	0.000000	0.05342	0.00015	0.00004	0.00001	0.05338	0.00015	0.00226	0.00001	*0.00739*	*0.00002*
Average 9	0.00000	0.000001	0.05322	0.00160			0.05374	0.00067	0.00192	0.00024	*0.00741*	*0.00015*
Session 10												
LA30222-0044	0.00000	0.000000	0.05252	0.00035	0.00000	0.00001	0.05252	0.00035	0.00205	0.00003	*0.00730*	*0.00003*
LA30222-0045	0.00001	0.000001	0.05399	0.00022	0.00012	0.00002	0.05389	0.00022	0.00219	0.00003	*0.00738*	*0.00004*
LA30222-0046	0.00000	0.000002	0.05386	0.00023	0.00007	0.00003	0.05380	0.00023	0.00218	0.00003	*0.00751*	*0.00002*
LA30222-0047	0.00000	0.000000	0.05375	0.00032	0.00000	0.00000	0.05375	0.00032	0.00218	0.00004	*0.00724*	*0.00003*
LA30222-0048	0.00000	0.000000	0.05487	0.00035	0.00000	0.00001	0.05487	0.00035	0.00219	0.00002	*0.00741*	*0.00005*
LA30222-0049	0.00000	0.000000	0.04976	0.00047	0.00000	0.00001			0.00174	0.00004	*0.00760*	*0.00004*
LA30222-0050	0.00000	0.000001	0.05264	0.00018	0.00005	0.00002	0.05260	0.00018	0.00221	0.00004	*0.00716*	*0.00002*
LA30222-0051	0.00000	0.000000	0.05432	0.00019	0.00000	0.00001	0.05432	0.00019	0.00227	0.00002	*0.00739*	*0.00002*
LA30222-0052	0.00001	0.000002	0.05365	0.00020	0.00010	0.00003	0.05357	0.00020	0.00226	0.00002	*0.00736*	*0.00002*
LA30222-0053	0.00000	0.000000	0.05014	0.00025	0.00000	0.00001			0.00199	0.00003	*0.00780*	*0.00007*
LA30222-0054	0.00000	0.000000	0.05329	0.00021	0.00000	0.00000	0.05329	0.00021	0.00199	0.00002	*0.00745*	*0.00006*
LA30222-0055	0.00000	0.000001	0.05346	0.00029	0.00003	0.00001	0.05343	0.00029	0.00215	0.00003	*0.00744*	*0.00003*
Average 10	0.00000	0.000002	0.05302	0.00157			0.05361	0.00071	0.00212	0.00015	*0.00742*	*0.00017*
Session 11												
n821-02a	0.00001	0.000001	0.05386	0.00011	0.00017	0.00001			0.00263	0.00003	0.00738	0.00002
n821-02b	0.00000	0.000001	0.05480	0.00012	0.00007	0.00001	0.05474	0.00012	0.00244	0.00004	0.00747	0.00002
n821-02c	0.00000	0.000000	0.05479	0.00011	0.00003	0.00001	0.05477	0.00011	0.00242	0.00003	0.00746	0.00003
n821-02d	0.00000	0.000000	0.05439	0.00015	0.00007	0.00001	0.05434	0.00015	0.00260	0.00003	0.00756	0.00002
n821-02e	0.00001	0.000001	0.05453	0.00013	0.00019	0.00002	0.05438	0.00013	0.00274	0.00004	0.00752	0.00002
n821-02f	0.00001	0.000001	0.05450	0.00011	0.00011	0.00002	0.05441	0.00011	0.00272	0.00004	0.00747	0.00003
n821-02g	0.00000	0.000001	0.05429	0.00015	0.00007	0.00001	0.05423	0.00015	0.00267	0.00003	0.00749	0.00003
Average 11	0.00001	0.000003	0.05445	0.00032			0.05448	0.00022	0.00260	0.00013	0.00748	0.00005
Session 12												
n821-02h	0.00000	0.000001	0.05581	0.00017	0.00007	0.00001			0.00237	0.00004	0.00746	0.00003
n821-02i	0.00000	0.000001	0.05448	0.00022	0.00006	0.00001	0.05443	0.00022	0.00250	0.00003	0.00749	0.00003
n821-02j	0.00002	0.000001	0.05496	0.00015	0.00040	0.00003	0.05464	0.00015	0.00320	0.00003	0.00750	0.00002
n821-02k	0.00000	0.000001	0.05432	0.00020	0.00004	0.00001	0.05429	0.00020	0.00249	0.00004	0.00752	0.00002
n821-02l	0.00001	0.000001	0.05447	0.00020	0.00013	0.00002	0.05437	0.00020	0.00251	0.00004	0.00740	0.00003
n821-02m	0.00003	0.000002	0.05438	0.00019	0.00059	0.00004	0.05390	0.00019	0.00369	0.00004	0.00744	0.00004
n821-02n	0.00000	0.000000	0.05433	0.00017	0.00003	0.00001	0.05430	0.00017	0.00298	0.00004	0.00748	0.00003
Average 12	0.00001	0.000012	0.05468	0.00054			0.05432	0.00024	0.00282	0.00049	0.00747	0.00004

Table A-3 (contd.)

File	204/206	±	207/206	±	f	±	207/206*	±	208/206	±	235/238	±
Session 13												
n821-02o	0.00001	0.000000	0.05674	0.00014	0.00010	0.00001			0.00266	0.00001	0.00793	0.00002
n821-02p	0.00000	0.000000	0.05523	0.00017	0.00001	0.00000	0.05522	0.00017	0.00245	0.00002	0.00799	0.00003
n821-02q	0.00000	0.000000	0.05511	0.00016	0.00001	0.00000	0.05510	0.00016	0.00264	0.00001	0.00786	0.00002
n821-02r	0.00000	0.000000	0.05504	0.00012	0.00008	0.00001	0.05497	0.00012	0.00281	0.00002	0.00786	0.00002
n821-02s	0.00000	0.000000	0.05504	0.00015	0.00009	0.00001	0.05497	0.00015	0.00244	0.00002	0.00793	0.00002
n821-02t	0.00001	0.000001	0.05514	0.00015	0.00024	0.00001	0.05495	0.00015	0.00253	0.00001	0.00776	0.00002
n821-02u	0.00001	0.000001	0.05540	0.00018	0.00013	0.00001	0.05530	0.00018	0.00227	0.00001	0.00786	0.00002
Average 13	0.00001	0.000004	0.05539	0.00061			0.05509	0.00015	0.00254	0.00018	0.00788	0.00008
Session 14												
n821-05a	0.00001	0.000001	0.05555	0.00014	0.00009	0.00001	0.05548	0.00014	0.00257	0.00002	0.00756	0.00002
n821-05b	0.00008	0.000004	0.05549	0.00018	0.00137	0.00006	0.05439	0.00018	0.00803	0.00019	0.00751	0.00003
n821-05c	0.00000	0.000000	0.05058	0.00015	0.00003	0.00000	0.05056	0.00015	0.00234	0.00002	0.00751	0.00002
n821-05d	0.00001	0.000001	0.05409	0.00014	0.00014	0.00001	0.05397	0.00014	0.00309	0.00001	0.00748	0.00002
n821-05e	0.00000	0.000000	0.05265	0.00018	0.00005	0.00001	0.05261	0.00018	0.00269	0.00001	0.00753	0.00002
n821-05f	0.00001	0.000001	0.05118	0.00012	0.00009	0.00001	0.05111	0.00012	0.00247	0.00002	0.00751	0.00002
n821-05g	0.00003	0.000002	0.05455	0.00016	0.00050	0.00004	0.05414	0.00016	0.00511	0.00012	0.00754	0.00002
n821-05h	0.00001	0.000001	0.05043	0.00018	0.00024	0.00002	0.05024	0.00018	0.00317	0.00002	0.00758	0.00002
Average 14	0.00002	0.000025	0.05307	0.00214			0.05281	0.00198	0.00368	0.00196	0.00753	0.00003
Session 15												
n821-05i	0.00000	0.000000	0.05090	0.00018	0.00000	0.00000	0.05090	0.00018	0.00255	0.00001	0.00756	0.00001
n821-05j	0.00000	0.000000	0.05384	0.00011	0.00000	0.00000	0.05384	0.00011	0.00263	0.00001	0.00755	0.00001
n821-05k	0.00000	0.000000	0.05254	0.00016	0.00000	0.00000	0.05254	0.00016	0.00245	0.00001	0.00752	0.00001
n821-05l	0.00001	0.000000	0.05333	0.00018	0.00010	0.00001	0.05325	0.00018	0.00227	0.00002	0.00752	0.00001
n821-05m	0.00000	0.000000	0.05226	0.00018	0.00009	0.00001	0.05219	0.00018	0.00213	0.00002	0.00749	0.00001
n821-05n	0.00000	0.000000	0.05167	0.00014	0.00000	0.00000	0.05167	0.00014	0.00263	0.00002	0.00753	0.00001
Average 15	0.00000	0.000003	0.05242	0.00107			0.05240	0.00106	0.00244	0.00020	0.00753	0.00002
Session 16												
n911-01f	0.00000	0.000000	0.04714	0.00041	0.00001	0.00000			0.00202	0.00002	0.00752	0.00001
n911-01g	0.00000	0.000000	0.05442	0.00009	0.00004	0.00001	0.05439	0.00009	0.00275	0.00002	0.00750	0.00001
n911-01h	0.00000	0.000000	0.05396	0.00012	0.00002	0.00000	0.05395	0.00012	0.00228	0.00002	0.00753	0.00001
n911-01i	0.00005	0.000005	0.05563	0.00016	0.00091	0.00010	0.05489	0.00016	0.00452	0.00023	0.00753	0.00001
Average 16	0.00002	0.000028	0.05279	0.00383			0.05441	0.00047	0.00318	0.00118	0.00752	0.00002
Session 17												
n911-01n	0.00001	0.000001	0.05425	0.00013	0.00012	0.00001	0.05415	0.00013	0.00258	0.00002	0.00755	0.00002
n911-01o	0.00002	0.000001	0.05440	0.00011	0.00027	0.00002	0.05418	0.00011	0.00231	0.00005	0.00752	0.00001
n911-01p	0.00001	0.000001	0.05447	0.00010	0.00012	0.00001	0.05437	0.00010	0.00257	0.00002	0.00752	0.00001
n911-01q	0.00006	0.000006	0.05547	0.00021	0.00102	0.00010	0.05465	0.00021	0.00362	0.00016	0.00752	0.00002
n911-01s	0.00000	0.000001	0.05435	0.00011	0.00009	0.00001	0.05428	0.00011	0.00242	0.00002	0.00753	0.00001
n911-01t	0.00000	0.000000	0.05438	0.00016	0.00003	0.00001	0.05436	0.00016	0.00245	0.00002	0.00753	0.00002
Average 17	0.00002	0.000021	0.05455	0.00045			0.05433	0.00018	0.00266	0.00048	0.00753	0.00001
Session 18a												
n911-03a	0.00000	0.000002	0.05484	0.00040	0.00007	0.00003	0.05478	0.00040	0.00220	0.00004	0.00746	0.00001
n911-03b	0.00000	0.000000	0.05383	0.00047	0.00000	0.00000	0.05383	0.00047	0.00223	0.00006	0.00744	0.00001
n911-03c	0.00001	0.000002	0.05423	0.00035	0.00022	0.00004	0.05405	0.00035	0.00253	0.00008	0.00747	0.00001
n911-03d	0.00000	0.000001	0.05360	0.00040	0.00004	0.00002	0.05357	0.00040	0.00239	0.00006	0.00744	0.00001
n911-03e	0.00000	0.000002	0.05433	0.00045	0.00009	0.00003	0.05426	0.00045	0.00198	0.00006	0.00744	0.00001
n911-03f	0.00000	0.000000	0.05360	0.00035	0.00000	0.00000	0.05360	0.00035	0.00215	0.00004	0.00744	0.00001
n911-03g	0.00001	0.000003	0.05405	0.00038	0.00018	0.00005	0.05390	0.00038	0.00278	0.00007	0.00747	0.00001
Average 18a	0.00000	0.000005	0.05407	0.00044			0.05400	0.00042	0.00232	0.00027	0.00745	0.00001
Session 18b												
n911-03h	0.00001	0.000001	0.05472	0.00024	0.00017	0.00002	0.05459	0.00024	0.00261	0.00003	0.00754	0.00002
n911-03i	0.00000	0.000000	0.05460	0.00012	0.00004	0.00001	0.05457	0.00012	0.00243	0.00003	0.00751	0.00002
n911-03j	0.00001	0.000001	0.05473	0.00013	0.00011	0.00001	0.05464	0.00013	0.00255	0.00003	0.00753	0.00002
Average 18b	0.00001	0.000004	0.05468	0.00007			0.05460	0.00004	0.00253	0.00009	0.00753	0.00002

Table A-3 (contd.)

File	204/206	±	207/206	±	f	±	207/206*	±	208/206	±	235/238	±
Session 19												
n911-06a	0.00001	0.000000	0.05412	0.00005	0.00013	0.00001	0.05402	0.00005	0.00224	0.00001	0.00754	0.00001
n911-06f	0.00001	0.000001	0.05377	0.00012	0.00010	0.00001	0.05369	0.00012	0.00206	0.00004	0.00758	0.00004
n911-06g	0.00000	0.000001	0.05423	0.00014	0.00006	0.00001	0.05418	0.00014	0.00241	0.00003	0.00755	0.00005
n911-06h	0.00000	0.000001	0.05421	0.00025	0.00005	0.00001	0.05417	0.00025	0.00239	0.00003	0.00761	0.00005
n911-06i	0.00001	0.000002	0.05418	0.00020	0.00024	0.00003	0.05398	0.00020	0.00274	0.00003	0.00759	0.00003
n911-06j	0.00001	0.000001	0.05405	0.00015	0.00020	0.00002	0.05389	0.00015	0.00255	0.00003	0.00756	0.00004
Average 19	0.00001	0.000004	0.05409	0.00017			0.05399	0.00018	0.00240	0.00023	0.00757	0.00002
Session 20												
n911-06k	0.00000	0.000000	0.05364	0.00017	0.00000	0.00000	0.05364	0.00017	0.00196	0.00003	0.00751	0.00001
n911-06l	0.00000	0.000003	0.05419	0.00020	0.00000	0.00005	0.05419	0.00020	0.00259	0.00007	0.00752	0.00001
n911-06m	0.00000	0.000000	0.05392	0.00019	0.00000	0.00000	0.05392	0.00019	0.00251	0.00007	0.00749	0.00001
n911-06n	0.00000	0.000000	0.05405	0.00022	0.00000	0.00000	0.05405	0.00022	0.00198	0.00003	0.00751	0.00002
n911-06o	0.00000	0.000000	0.05366	0.00024	0.00000	0.00000	0.05366	0.00024	0.00234	0.00007	0.00750	0.00002
Average 20	0.00000	0.000000	0.05389	0.00024			0.05389	0.00024	0.00227	0.00029	0.00750	0.00001

Table A-4. Masses 209 and 239 measured by SIMS in uraninite P88 and LAMNH-30222. Errors are 1σ.

P88					LAMNH				
File	209/206	±	239/238	±	File	209/206	±	239/238	±
Session OR-1									
1-3PB6	0.000077	0.000001	0.00041	0.000003	1-3PB1	0.000182	0.000003	0.00191	0.00001
1-3PB7	0.000077	0.000001	0.00096	0.000007	1-3PB2	0.000078	0.000001	0.00177	0.00001
1-3PB8	0.000074	0.000001	0.00094	0.000007	1-3PB3	0.000070	0.000001	0.00179	0.00001
1-3PB9	0.000072	0.000000	0.00082	0.000007	1-3PB4	0.000070	0.000002	0.00167	0.00001
1-3PB10	0.000074	0.000001	0.00089	0.000009	1-3PB5	0.000071	0.000001	0.00190	0.00001
Average 1	0.000075	0.000002	0.00080	0.000226		0.000094	0.000049	0.00181	0.00010
Session OR-2									
1-4PB12	0.000076	0.000001	0.00087	0.000009	1-4PB6	0.000119	0.000007	0.00179	0.00002
1-4PB13	0.000075	0.000001	0.00094	0.000012	1-4PB7	0.000207	0.000002	0.00197	0.00001
1-4PB14	0.000077	0.000001	0.00088	0.000011	1-4PB8			0.00151	0.00001
1-4PB15	0.000076	0.000001	0.00084	0.000009	1-4PB9	0.000226	0.000003	0.00176	0.00001
1-4PB16	0.000077	0.000001	0.00087	0.000014	1-4PB10	0.000200	0.000004	0.00212	0.00002
					1-4PB11	0.000217	0.000003	0.00151	0.00001
Average 2	0.000076	0.000001	0.00088	0.000036		0.000194	0.000043	0.00178	0.00024
Session OR-3									
1-5PB1	0.000074	0.000001	0.00081	0.000011	1-5PB6	0.000198	0.000002	0.00182	0.00002
1-5PB2	0.000087	0.000001	0.00080	0.000009	1-5PB7	0.000106	0.000002	0.00173	0.00001
1-5PB3	0.000083	0.000001	0.00076	0.000007	1-5PB8	0.000159	0.000001	0.00175	0.00001
1-5PB4	0.000078	0.000001	0.00095	0.000008	1-5PB9	0.000053	0.000001	0.00184	0.00002
1-5PB5	0.000080	0.000001	0.00076	0.000008	1-5PB10	0.000214	0.000002	0.00195	0.00001
Average 3	0.000080	0.000005	0.00082	0.000079		0.000146	0.000066	0.00182	0.00009
Session 16									
n911-02a	0.000079	0.000001	0.00256	0.000084	n911-01f	0.000078	0.000003	0.00499	0.00002
n911-02e	0.000068	0.000001	0.00324	0.000058	n911-01g	0.000073	0.000002	0.00401	0.00003
n911-02f	0.000070	0.000001	0.00243	0.000088	n911-01h	0.000042	0.000001	0.00390	0.00003
n911-02g	0.000070	0.000001	0.00243	0.000068	n911-01i	0.000186	0.000008	0.00407	0.00003
Average 16	0.000072	0.000005	0.00267	0.000390		0.000095	0.000063	0.00424	0.00050
Session 17									
n911-02h	0.000077	0.000001	0.00159	0.000077	n911-01n	0.000093	0.000002	0.00302	0.00003
n911-02l	0.000067	0.000000	0.00169	0.000035	n911-01o	0.000066	0.000004	0.00307	0.00002
n911-02m	0.000071	0.000001	0.00172	0.000041	n911-01p	0.000065	0.000002	0.00307	0.00004
n911-02n	0.000066	0.000001	0.00149	0.000065	n911-01q	0.000171	0.000008	0.00296	0.00004
n911-02o	0.000069	0.000001	0.00142	0.000042	n911-01s	0.000145	0.000003	0.00312	0.00003
n911-02p	0.000071	0.000000	0.00143	0.000033	n911-01t	0.000080	0.000002	0.00298	0.00002
Average 17	0.000070	0.000004	0.00156	0.000131		0.000103	0.000045	0.00304	0.00006
Session 18 a									
n911-04a	0.000047	0.000002	0.00134	0.000024	n911-03a	0.000038	0.000003	0.00191	0.00001
n911-04b	0.000061	0.000002	0.00112	0.000027	n911-03b	0.000040	0.000004	0.00166	0.00001
n911-04c	0.000059	0.000002	0.00119	0.000027	n911-03c	0.000050	0.000004	0.00192	0.00001
n011-04d	0.000062	0.000003	0.00118	0.000018	n911-03d	0.000051	0.000004	0.00166	0.00001
n911-04f	0.000060	0.000002	0.00113	0.000024	n911-03e	0.000093	0.000006	0.00164	0.00001
n911-04g	0.000056	0.000002	0.00106	0.000030	n911-03f	0.000076	0.000005	0.00180	0.00001
n911-04h	0.000061	0.000002	0.00108	0.000018	n911-03g	0.000030	0.000004	0.00166	0.00001
Average 18a	0.000058	0.000005	0.00116	0.000093		0.000054	0.000022	0.00175	0.00012
Session 18b									
n911-04i	0.000068	0.000000	0.00170	0.000081	n911-03h			0.00402	0.00004
n911-04j	0.000070	0.000001	0.00162	0.000053	n911-03i	0.000083	0.000001	0.00369	0.00005
n911-04k	0.000071	0.000001	0.00182	0.000067	n911-03j	0.000074	0.000002	0.00363	0.00003
Average 18b	0.000069	0.000002	0.00171	0.000103		0.000079	0.000006	0.00378	0.00021

Table A-4 (contd.)

P88 File	209/206	±	239/238	±	LAMNH File	209/206	±	239/238	±
Session 19									
n911-07a	0.000066	0.000001			n911-06a	0.000061	0.000001	0.00194	0.00001
n911-07f	0.000057	0.000001	0.00146	0.000021	n911-06f	0.000102	0.000007	0.00241	0.00010
n911-07g	0.000063	0.000001	0.00137	0.000033	n911-06g	0.000059	0.000002	0.00227	0.00007
n911-07h	0.000068	0.000001	0.00118	0.000036	n911-06h	0.000229	0.000006	0.00205	0.00005
n911-07i	0.000062	0.000001	0.00141	0.000019	n911-06i			0.00233	0.00005
n911-07j	0.000062	0.000001	0.00125	0.000031	n911-06j	0.000131	0.000003	0.00207	0.00004
Average 19	0.000063	0.000004	0.00133	0.000113		0.000116	0.000070	0.00218	0.00018
Session 20									
n911-07k	0.000056	0.000002	0.00097	0.000014	n911-06k	0.000022	0.000003	0.00102	0.00001
n911-07l	0.000057	0.000002	0.00094	0.000008	n911-06l	0.000053	0.000003	0.00095	0.00002
n911-07m	0.000056	0.000003	0.00093	0.000015	n911-06m	0.000065	0.000003	0.00108	0.00001
n911-07n	0.000048	0.000002	0.00092	0.000017	n911-06n	0.000017	0.000002	0.00113	0.00001
					n911-06o	0.000056	0.000003	0.00116	0.00001
Average 20	0.000054	0.000004	0.00094	0.000021		0.000042	0.000022	0.00107	0.00009